PHYSICAL REVIEW D VOLUME 53, NUMBER 11 1 JUNE 1996

Signals for minimal supergravity at the CERN Large Hadron Collider. II. Multilepton channels

Howard Baer,[1] Chih-hao Chen,[2] Frank Paige,[3] and Xerxes Tata[4,1]
[1]*Department of Physics, Florida State University, Tallahassee, Florida 32306*
[2]*Department of Physics, University of California, Davis, California 95616*
[3]*Brookhaven National Laboratory, Upton, New York 11973*
[4]*Department of Physics and Astronomy, University of Hawaii, Honolulu, Hawaii 96822*
(Received 21 December 1995)

We use ISAJET to perform a detailed study of the multilepton signals expected from cascade decays of supersymmetric particle produced at the CERN LHC. Our analysis is performed within the framework of the minimal supergravity model with gauge coupling unification and radiative electroweak symmetry breaking. We delineate the regions of parameter space where jets plus missing energy plus 1, 2 (opposite-sign and same-sign dileptons), and 3 isolated lepton events should be visible above standard model backgrounds. We find that if any $\not{E}_T$ signal at the LHC is to be attributed to gluino and/or squark production, and if $m_{\tilde{g}} \lesssim 1$ TeV, then several of these signals must be simultaneously observable. Furthermore, assuming 10 fb^{-1} of integrated luminosity, we find that the reach for supersymmetry in the $1\ell + \text{jets} + \not{E}_T$ channel extends to $m_{\tilde{g}} \sim 2300(1600)$ GeV for $m_{\tilde{q}} \sim m_{\tilde{g}}$ ($m_{\tilde{q}} \sim 1.5 m_{\tilde{g}}$), and exceeds the corresponding reach in the $0\ell + \not{E}_T$ channel. We show that measurements of the various topological cross sections, jet, and B-hadron multiplicities in these events, together with the charge asymmetry for single lepton and same-sign dilepton events, and flavor asymmetry for opposite-sign dilepton events, serve to narrow the allowed range of underlying SUGRA parameter values. We also delineate parameter regions where signals with clean isolated dilepton (from slepton production) and trilepton events (from chargino or neutralino production) are visible at the LHC, and examine the extent to which these signals can be separated from other SUSY sources. [S0556-2821(96)01011-9]

PACS number(s): 14.80.Ly, 11.30.Pb, 13.85.Qk

I. INTRODUCTION AND MOTIVATION

The search for supersymmetric particles is now an integral part of all current, as well as future, experimental programs at high energy colliders. Aside from the many attractive features of supersymmetry (SUSY), the impetus for these searches comes from the fact that weak scale SUSY [1], which is introduced to ameliorate the fine-tuning problem of the standard model (SM), requires that the supersymmetric partners of SM particles *must* be accessible to experiments that probe the TeV energy scale. Thus, while experiments at the CERN e^+e^- collider LEP 2 and at the Fermilab Tevatron (or its upgrades) may well discover sparticles, a definitive search for supersymmetry can only be performed [2] at supercolliders such as the CERN Large Hadron Collider (LHC) or at electron-positron linear colliders with $\sqrt{s} = 500$–1500 GeV. There is a general agreement, based on detailed studies of SUSY signals both within the more general minimal supersymmetric model (MSSM) framework [3–6] as well as within the very attractive and economic supergravity (SUGRA) [7] grand unified theory (GUT) framework [8–11], that weak scale SUSY will not evade detection at these facilities [12].

The natural question then is the following: If we do see signals for new physics, can we unravel their origin, and trace them to the production of supersymmetric particles? At electron-positron colliders, where the cleanliness of the interaction environment allows for the precision measurements [14,8,9,15] of at least some of the properties of these particles (mass, spin, decay patterns, ...), this may be a straightforward exercise, especially if the machine energy is increased incrementally, so that it is possible to focus on just one new signal at a time. At the LHC, however, the situation is much more complicated, not only because of the messier environment, but also because *all* new particles which are kinematically accessible will simultaneously contribute to the signal: we will thus have the additional task of sorting the supersymmetric signals from one another in order to discover the nature of the new physics.

Some progress has already been made on the issue of identifying the sparticle production processes that give rise to SUSY signals at the LHC. For instance, it has been shown [16] that, with suitable cuts, the clean $3\ell + \not{E}_T$ signal from the production of charginos and neutralinos via the reaction $pp \to \widetilde{W}_1\widetilde{Z}_2 \to \ell\nu\widetilde{Z}_1 + \ell'\overline{\ell'}\widetilde{Z}_1$ cannot only be separated from SM backgrounds, but also, that it can be isolated from other SUSY sources. An observation of a signal in this channel would, therefore, unambiguously point to $\widetilde{W}_1\widetilde{Z}_2$ production as its source, at least within the SUSY framework. It is, however, not always possible to devise cuts to isolate a single source of SUSY events. A detailed study of the signal characteristics may then help to identify the sparticles producing the signal. In a previous study [11], hereafter referred to as paper I, we examined the reach of the LHC in the multijet plus $\not{E}_T$ channel and studied what information could be obtained by a detailed study of this sample. Assuming as usual that squarks cannot be much lighter than gluinos, we showed that if gluinos are lighter than about 750 GeV, their mass could be extracted to 15–25 % by reconstructing multijet masses in opposite detector hemispheres. Furthermore, by measuring the mean jet multiplicity $\langle n_j \rangle$, which is ob-

servably larger if squarks are much heavier than gluinos, it should be possible to distinguish the $m_{\tilde{q}} \simeq m_{\tilde{g}}$ case from the one where squarks are substantially heavier than gluinos. While the gluino mass would determine $m_{1/2}$, $\langle n_j \rangle$ will at least enable us to decide whether m_0 is small or comparable to $m_{1/2}$, or much larger.

Are there other ways by which we can tell what is being produced at the LHC? Also, is it possible to test whether the minimal SUGRA framework adopted in paper I (as well as in many recent phenomenological analyses [8,9,17–23] of SUSY) can consistently account for all the observed signals, or whether some of the underlying assumptions about the symmetries of physics at the ultrahigh scale need to be modified? It has already been shown [8,9] that the precision measurements that are possible in the clean environment of e^+e^- collisions will allow experimentalists to perform incisive tests of the SUGRA framework at future linear colliders. While it is not possible to perform similar measurements at hadron colliders, the big advantage of the LHC over 500 GeV linear colliders is that many more sparticle production processes should be kinematically accessible, resulting in a large number of potential observables. Since the minimal SUGRA GUT model with radiative breaking of electroweak symmetry is completely fixed by just four SUSY parameters: m_0 and $m_{1/2}$, the universal scalar mass and gaugino masses at the high scale $M_X \sim M_{\rm GUT}$, the SUSY-breaking universal trilinear coupling A_0, and the parameter $\tan\beta$ along with $\mathrm{sgn}\mu$, the consistency of the framework can be tested by verifying that the rates and distributions in all the observed channels can be accommodated by a single choice of model parameters. Even more ambitiously, one could ask whether it would be possible to determine the underlying parameters from the observed signals, and we report the results of our preliminary attempt to do so in this paper.

We stress here that we do not mean to imply that the SUGRA framework is the uniquely correct one. Indeed, the sensitivity to the details of its predictions should be examined, particularly when studying the reach of future facilities. Nonetheless, it is an economic, attractive, and predictive framework, and it can be used as a guide for sparticle masses and mixing patterns. Such a framework is needed since without assuming anything other than the weak scale symmetries, there are far too many parameters, making phenomenological analyses intractable.

It should be clear from the preceding discussion that a study of all possible signals as a function of SUGRA parameters is a first step toward testing the model framework at the LHC. Of course, it is equally important to quantify the reach of the LHC in each of these channels which include the nonleptonic $\not{E}_T$+jets channel studied in paper I, the 1ℓ+jets+$\not{E}_T$ channel, the opposite-sign (OS) dilepton+jets+$\not{E}_T$ channel, the same-sign (SS) dilepton+jets+$\not{E}_T$ channel, and the multilepton+jets+$\not{E}_T$ channel, with $n_\ell \geq 3$.

These signal channels ought to originate mainly from squark and gluino pair production, followed by their cascade decays. In addition, there are also clean (i.e., free from central jet activity) channels with dilepton plus $\not{E}_T$ events, and trilepton and $n_\ell \geq 4$ lepton events, mainly from the pair production of sleptons [24,25] as well as from $\widetilde{W}_1\widetilde{W}_1$, $\widetilde{W}_1\widetilde{Z}_2$ [26,16], and $\widetilde{Z}_2\widetilde{Z}_2$ [27] production processes. Of course, after cuts, several sparticle production mechanisms can contribute to each channel, so that it is necessary to simultaneously generate the production of *all* sparticles in order to obtain an accurate assessment of the expected signals.

In this paper we continue the study of SUSY signals within the SUGRA framework that we began in paper I. We use ISAJET 7.14 [28] to compute [29] the signal cross sections after cuts designed to separate the SUSY signals from SM backgrounds, and wherever possible, also to separate SUSY sources from one another, in each of the leptonic channels listed above. We show these in the m_0-$m_{1/2}$ plane, which provides a convenient way to display the signals from different sparticle production processes. For other parameters, our canonical choices are $A_0=0$, $\tan\beta=2$ and 10, and we adopt both signs of μ. To orient the reader with various sparticles masses derived from the SUGRA framework, we show contours of squark and gluino masses in Fig. 1, and of slepton and chargino masses in Fig. 2, for (a) $\tan\beta=2$, $\mu<0$, (b) $\tan\beta=2$, $\mu>0$, (c) $\tan\beta=10$, $\mu<0$, and (d) $\tan\beta=10$, $\mu>0$. We remind the reader of the approximate relationship $m_{\widetilde{Z}_2} \simeq m_{\widetilde{W}_1} \simeq 2m_{\widetilde{Z}_1}$ that usually holds because $|\mu|$ tends to be large within this framework. In Fig. 1, as well as in many subsequent figures, the regions shaded by bricks (hatches) are excluded by theoretical (experimental) constraints as discussed in paper I. The gluino mass contours in Fig. 1 are not exactly horizontal because of the difference [30] between the running and physical (i.e., pole) gluino mass. In Fig. 2, we also show the region where the ''spoiler'' decay modes $\widetilde{Z}_2 \to \widetilde{Z}_1 H_\ell$ or $\widetilde{Z}_2 \to \widetilde{Z}_1 Z$ are kinematically accessible (above the dotted contours); in this region, leptonic decays of the $\widetilde{Z}_2$ are either very suppressed, or have additional backgrounds from SM Z boson production.

We map out the regions of parameter space where these signals are observable at the LHC, and compare this with the region that can be probed via the $\not{E}_T$ channel [11,6] as delineated in paper I. On the issue of the LHC reach, our main new result is that the 1ℓ channel provides the greatest reach for supersymmetry. However, the observation of signals in several channels is important, since it can help to identify SUSY as the unique source of new physics. We study jet and B-hadron multiplicity distributions, as well as charge asymmetry distributions in the single lepton and SS dilepton+jets+$\not{E}_T$ channels, and dilepton flavor asymmetry in the OS dilepton+jets+$\not{E}_T$ channel as these can provide information about the cascade decay chains of gluinos and squarks [17]. We also identify regions of parameter space where the clean trilepton and the clean OS, same-flavor dilepton signals are observable. While these regions form a subset of the region where SUSY may be probed via the multijet channels, an observation of these signals will be important because they will signal $\widetilde{W}_1\widetilde{Z}_2$ and slepton production, respectively; i.e., with suitable cuts described below, there is limited contamination from other SUSY sources.

In order to obtain a feel for the variation of the various signals with model parameters, we have for the most part presented our results in the m_0-$m_{1/2}$ plane for the cases (a)–(d) introduced above. While this will be important to those interested in detailed studies, the reader who is not concerned with the details of this variation could focus on just one of these cases, and simply refer to Fig. 18 where the

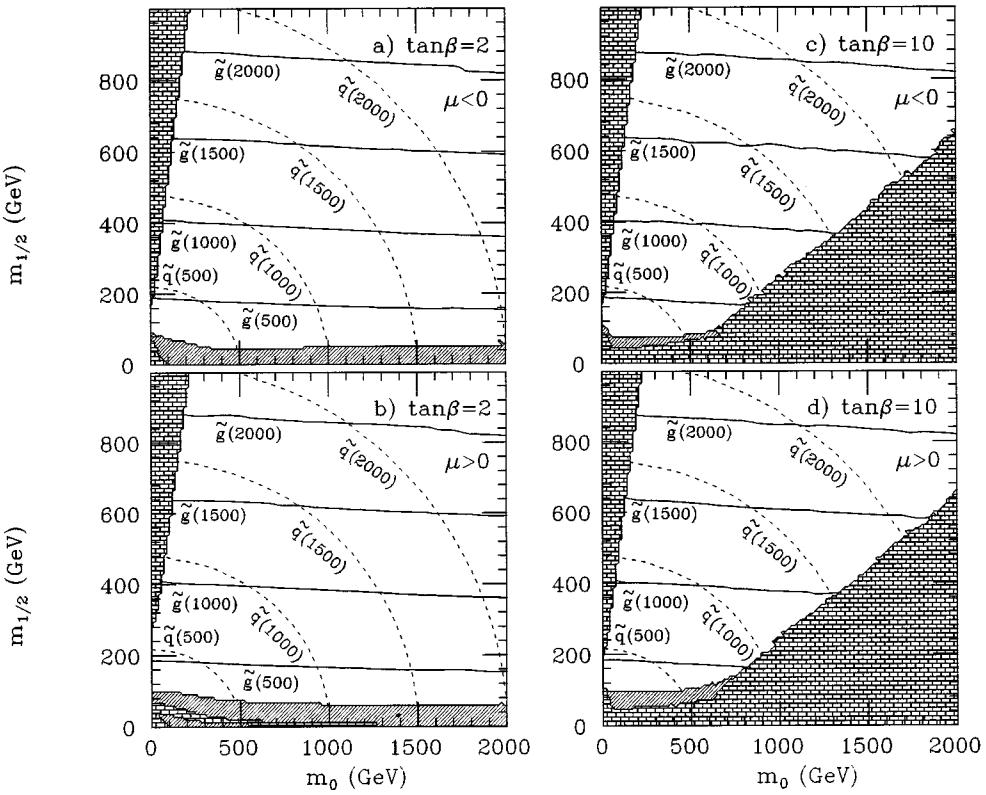

FIG. 1. Contour plots of squark and gluino masses in the m_0–$m_{1/2}$ plane of the minimal SUGRA model. Frames are shown for (a) $\tan\beta=2$, $\mu<0$, (b) $\tan\beta=2$, $\mu>0$, (c) $\tan\beta=10$, $\mu<0$, and (d) $\tan\beta=10$, $\mu>0$. We take $m_t=170$ GeV and $A_0=0$. The bricked regions are excluded by theoretical constraints discussed in paper I, while the shaded regions are excluded by experiment.

LHC reach in various channels is summarized for all four cases. The rest of this paper is organized as follows. In the next section, we briefly discuss some computational details. Sections III and IV focus on the multilepton plus multijet and clean multilepton channels, respectively. We present a comparative analysis of the reach in various channels in Sec. V, and also consolidate the information about the underlying SUGRA model parameters that might be obtained by study-

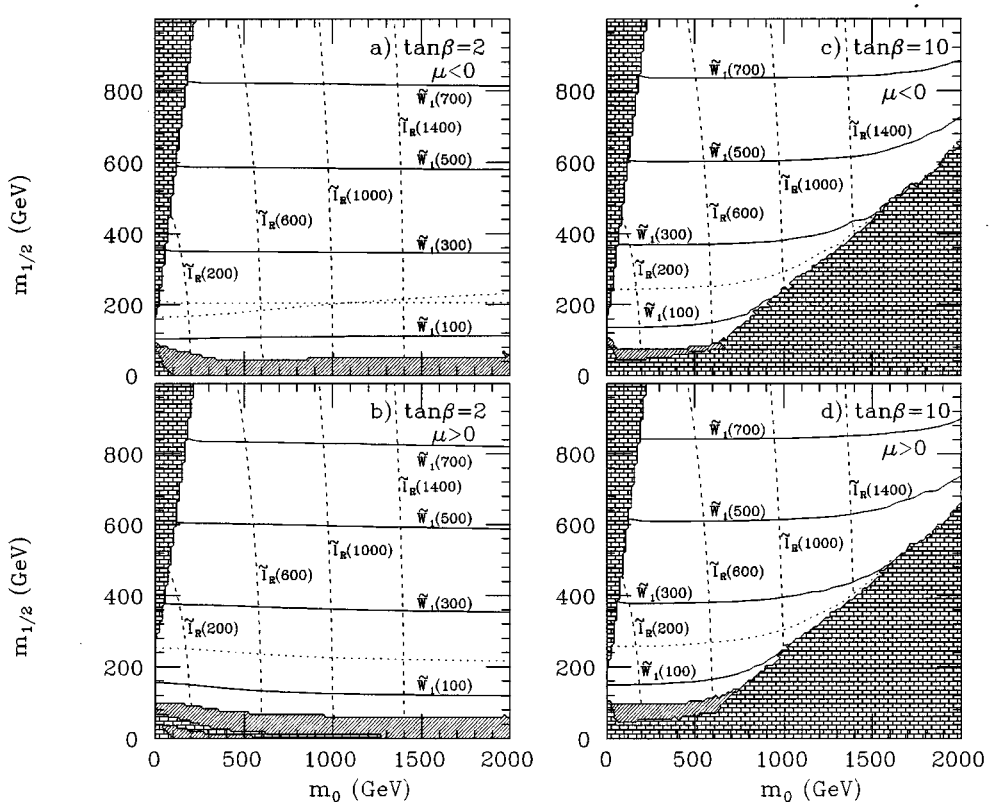

FIG. 2. Same as Fig. 1, except we plot contours of lightest chargino mass and contours of right slepton mass. Also shown by dotted contours are the kinematic limits for the neutralino spoiler decay modes, above which the decays $\tilde{Z}_2\to\tilde{Z}_1 H$ or $\tilde{Z}_2\to\tilde{Z}_1 Z$ are kinematically allowed.

ing distributions in these various channels.

II. EVENT SIMULATION

We work within the framework of the minimal SUGRA model and use ISAJET 7.14 to simulate the various leptonic signals for SUSY listed above. The implementation of the SUGRA framework into ISAJET has been described elsewhere [20,11] and will not be repeated here. We generate *all* lowest order $2\to2$ SUSY subprocesses in our simulation of the multilepton plus multijet signals (except for s-channel Higgs boson-mediated subprocesses). However, for the simulation of the *clean* multilepton signals, we have generated only slepton and chargino or neutralino events, since gluino and squark decays will very seldom yield final states without central jet activity [31].

For detector simulation at the LHC, we use the toy calorimeter simulation package ISAPLT. We simulate calorimetry covering $-5<\eta<5$ with cell size $\Delta\eta\times\Delta\phi=0.05\times0.05$. We take the hadronic energy resolution to be $50\%/\sqrt{E}\oplus0.03$ for $|\eta|<3$, where $\oplus$ denotes addition in quadrature, and to be $100\%/\sqrt{E}\oplus0.07$ for $3<|\eta|<5$, to model the effective p_T resolution of the forward calorimeter including the effects of shower spreading, which is otherwise neglected. We take electromagnetic resolution to be $10\%/\sqrt{E}\oplus0.01$. Although we have included these resolutions, which are typical of ATLAS [6] and CMS [32], we have made no attempt to estimate the effects of cracks, edges, and other problem regions. Much more detailed detector simulations are needed to understand the effects of such regions and of the resulting non-Gaussian tails, particularly on the $\not{E}_T$ resolution.

Jets are found using fixed cones of size $R=\sqrt{\Delta\eta^2+\Delta\phi^2}=0.7$ using the ISAJET routine GETJET. Clusters with $E_T>100$ GeV and $|\eta(\text{jet})|<3$ are labeled as jets. However, for the purpose of jet veto only, clusters with $E_T>25$ GeV and $|\eta(\text{jet})|<3$ are regarded as jets. Muons and electrons are classified as isolated if they have $p_T>10$ GeV, $|\eta(\ell)|<2.5$, and the visible activity within a cone of $R=0.3$ about the lepton direction is less than $E_T(\text{cone})=5$ GeV.

We assume an integrated luminosity of 10 fb^{-1}, corresponding to 10^{33} cm^{-2} s^{-1} for one year. Hence, we feel justified in neglecting the effects of pileup. We presume it would be possible to use the maximum LHC luminosity, 10^{34} cm^{-2} s^{-1}, to search for gluinos and squarks with masses $\gtrsim1$–2 TeV.

III. MULTILEPTON PLUS MULTIJET SIGNALS FOR SUPERSYMMETRY

A. Classification of signals and event selection

For $m_{\tilde g}$, $m_{\tilde q}\lesssim1$ TeV, $\tilde g\tilde g$, $\tilde g\tilde q$, and $\tilde q\tilde q$ production is the dominant source of SUSY events at the LHC. These production mechanisms, together with $\tilde g$ and $\tilde q$ cascade decays, naturally lead to events with n leptons$+m$ jets$+\not{E}_T$, where typically $n=0$–4 and $m\geq2$. These event topologies may also arise from the production of gluinos and squarks in association with a chargino or a neutralino. In addition, direct production of charginos, neutralinos, and sleptons followed by cascade decays to $\widetilde W_i$ or $\widetilde Z_j$ can lead to similar events.

Although in our simulation we generate all SUSY processes using ISAJET, our cuts are designed to selectively pick out gluino and squark events, whose characteristics are high transverse momentum jets and large missing transverse energy. Furthermore, the p_T of the primary jets from gluinos, as well as the $\not{E}_T$, are expected to scale with $m_{\tilde g}$. In contrast, the momenta of leptons, produced far down in the cascade decay chain from chargino and neutralino daughters, will not scale in energy the same way as jets and $\not{E}_T$ which can be produced in the first step of the cascade decay. Thus, following paper I, for the multilepton plus multijet signals for SUSY, we vary the missing-energy and jet-E_T cuts using a parameter E_T^c but fix the lepton cuts: Jet multiplicity, $n_{\text{jet}}\geq2$ (with $E_{T,\text{jet}}>100$ GeV), transverse sphericity $S_T>0.2$, and $E_T(j_1),E_T(j_2)>E_T^c$ and $\not{E}_T>E_T^c$.

We classify the events by the multiplicity of *isolated* leptons, and in the case of dilepton events, we also distinguish between the OS and the SS samples as these could have substantially different origins. For the leptons we require $p_T(\ell)>20$ GeV ($\ell=e$ or μ) and $M_T(\ell,\not{E}_T)>100$ GeV for the 1ℓ signal, and $p_T(\ell_1,\ell_2)>20$ GeV for $n=2,3,\ldots$ lepton signals. We do not impose any $p_T(\ell)>E_T^c$ requirement on the leptons for reasons explained above.

B. Calculation of backgrounds

SM processes, particularly those involving the production of heavy particles such as the W and Z bosons, or the top quarks, can mimic the leptonic signals listed above. We have used ISAJET to evaluate the following SM backgrounds to these signals: (1) tt production, where the leptonic decays of the tops can give up to two isolated leptons; for $n>2$ the additional lepton may come from a b or c decay or from the fragmentation of additional jets in the event, where the lepton is accidentally isolated; (2) W and Z boson + jet production, where additional jets and/or leptons come from parton showering; (3) WW, WZ, and ZZ production, where additional jets can again arise from QCD radiation; (4) QCD jet production, where leptons can arise from decays of heavy flavors produced directly or via gluon splitting.

ISAJET includes higher order QCD and electroweak effects in the branching approximation; i.e., it includes quark and gluon as well as weak vector boson radiation, using exact kinematics but only collinear dynamics. Thus, extra leptons can arise in any of the above hard scattering subprocesses additionally from, for instance, gluon splitting to top- or bottom-quark pairs, followed by their subsequent decays, or by W and Z boson radiations.

The E_T^c dependence of these background cross sections, obtained using CTEQ2L parton distributions [33], is displayed in Fig. 3 for (a) $1\ell+$jets events, (b) OS dilepton+ jets events, (c) SS dilepton+jets events, and (d) $3\ell+$jets events. We see that $W+$jets production is generally the largest background, except in the OS dilepton channel where the tt background dominates for modest values of E_T^c. Gauge boson pair production and QCD background sources are essentially negligible, compared to backgrounds from W, Z, and tt production. The multilepton background from gauge boson pair production is strongly suppressed, presumably because of the requirement of two additional hard jets as well as $\not{E}_T>E_T^c$.

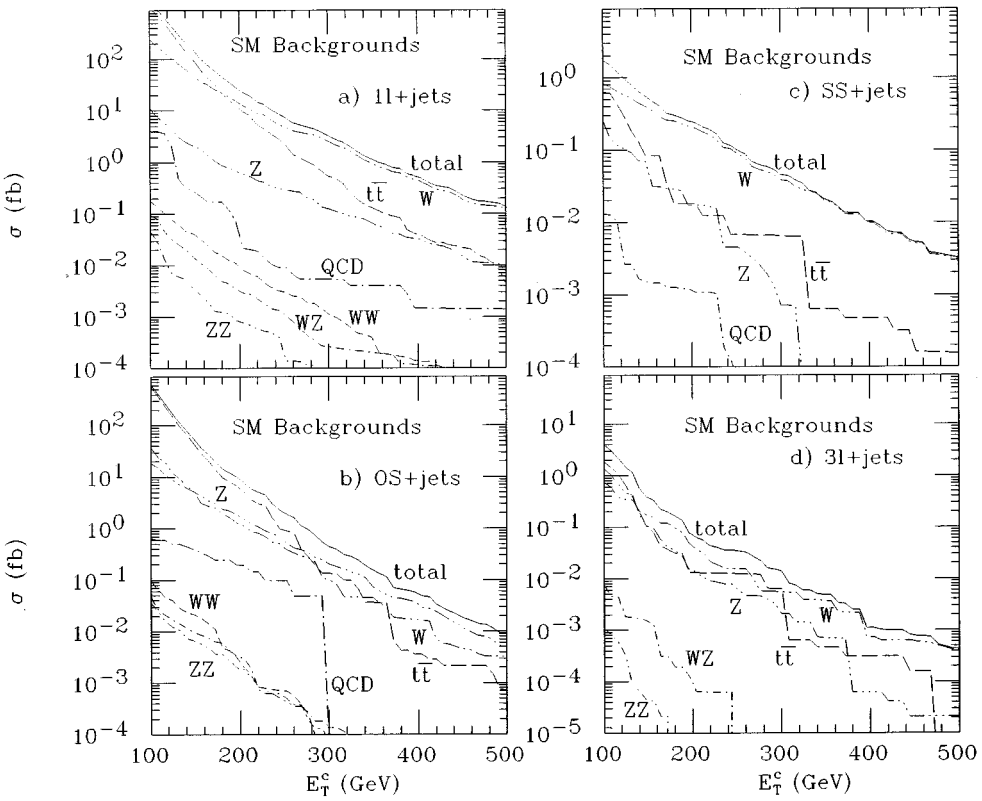

FIG. 3. SM backgrounds to various SUSY-search-event topologies in fb, after cuts, but as a function of the cut parameter E_T^c defined in the text. We show frames for (a) 1ℓ + jets events, (b) OS dilepton + jets events, (c) SS dilepton + jets events, and (d) 3ℓ + jets events.

The wiggles in the curves in Fig. 3 are a reflection of the statistical fluctuations in our simulation. We see that for modest values of E_T^c, the fluctuations in the biggest backgrounds are under control. We will see later that in order to extract the reach, we use $E_T^c = 200$ GeV in all but the 1ℓ channel for which we use $E_T^c = 400$ GeV. We have checked that for these ranges we typically obtain at least several tens of events passing the cuts in our simulation, so that the statistical errors on the relevant background estimates are in control. It should, of course, be remembered that our background calculations are probably correct only to a factor ~ 2–3 because of the inherent uncertainties associated with leading-log QCD, the parton shower approximation, our idealistic detector simulation, etc.

In order to enable the reader to assess this calculation, we have shown the details of the background calculation in the various multilepton channels in Table I for one value of E_T^c. Since only a tiny fraction of the events generated pass the cuts, it is necessary to generate events in several ranges of hard scattering p_T ($p_T^{\rm HS}$) for each SM process, and then combine these to obtain the background cross section from each of these sources [34]. The results of our computation for $E_T^c = 200$ GeV are shown in Table I for the 1ℓ, OS, SS, and 3ℓ signals. In those $p_T^{\rm HS}$ bins where we obtain no event, the bound shown corresponds to the cross section corresponding to the one-event level. We see that for the $t\bar{t}$ and W or Z backgrounds, which are the largest contributors to the background cross section, the main contribution indeed comes from the intermediate values of $p_T^{\rm HS}$, ensuring that we do have a reasonable estimate for the cross section. We have also checked that for the major contributors to the background, we have ten to several hundred events passing the cuts in our simulation, so that our estimates should be reliable to a few tens of percent, and frequently much better, as far as statistical errors are concerned. Finally, we see that the QCD background to the 1ℓ cross section is clearly small; while we typically obtain only a bound on this from our simulation, it is reasonable to expect that this will not be a substantial background in the multilepton channels.

We have also attempted to estimate the 4ℓ background with ISAJET. Such events, however, form an extremely tiny fraction of the total cross section so that a reliable simulation of these would require lengthy computer runs. Our simulation in which just a handful of events pass the cuts in each of the W+jets, Z+jets, and the $t\bar{t}$ channels, yields a cross section $\sigma(4\ell) = 0.04$ fb for this background for $E_T^c = 100$ GeV, which falls to 0.002 fb for $E_T^c = 200$ GeV. Even allowing for uncertainties in our estimates, we see that the SM background is essentially negligible. For reasons of brevity and because these signals are observable only for limited ranges of parameters, we have not shown these cross sections in the figures or in Table I.

C. SUSY multilepton plus multijet signals at the LHC

Our next goal is to evaluate the various SUSY n-lepton+m-jets+$\not{E}_T$ signals expected from supersymmetry at the LHC, and compare against background expectations. Toward this end, we show the signal cross sections along with the total SM background as a function of E_T^c in Fig. 4 for (a) 1ℓ+jets events, (b) OS dilepton+ jets events, (c) SS dilepton+jets events, and (d) 3ℓ+jets events. Our total signal and background cross sections are evaluated, as usual, at leading-log level, and so are uncertain to about a factor of 2; next-to-leading log gluino and squark cross sections can be found in Ref. [35]. We have illustrated the signal for the

TABLE I. Results of background calculation in fb after cuts using cut parameter $E_T^c = 200$ GeV. We list the hard scattering p_T ($p_T^{\rm HS}$) ranges over which the background processes were evaluated, and then the backgrounds from various SM processes. The upper bounds quoted correspond to the one-event level. We take $m_t = 170$ GeV.

$p_T^{\rm HS}$	$t\bar{t}$	QCD	W+jets	Z+jets	$WW+WZ+ZZ$
1ℓ					
50–100	<0.64	<391	<4.8	<0.74	<0.07
100–200	<1.0	<26	<1.0	<0.17	<0.02
200–400	3.7	<1.5	7.8	0.26	<0.003
400–800	7.2	<0.05	5.7	0.33	0.011
800–1600	0.42	0.02	0.39	0.02	0.002
1600–3200	0.001	0.0004	0.004	0.0	0.0
OS					
50–100	<0.64	<391	<4.8	<0.74	<0.07
100–200	1.0	<26	<1.0	<0.17	<0.02
200–400	2.6	<1.5	0.61	1.0	<0.003
400–800	2.1	0.19	0.52	0.63	0.011
800–1600	0.06	0.001	0.02	0.01	0.002
1600–3200	0.0	0.0001	0.001	0.0	0.0
SS					
50–100	<0.04	<391	<0.42	<0.35	<0.07
100–200	<0.05	<26	<0.08	<0.08	<0.02
200–400	<0.02	<1.5	0.09	0.009	<0.003
400–800	0.02	<0.05	0.11	0.007	<0.0004
800–1600	0.001	<0.001	0.009	0.0002	0.0
1600–3200	0.0	0.0	0.0	0.0	0.0
3ℓ					
50–100	<0.04	<391	<0.42	<0.35	<0.07
100–200	<0.05	<26	<0.08	<0.08	<0.02
200–400	<0.02	<1.5	0.02	<0.009	<0.003
400–800	0.01	<0.05	0.03	0.01	<0.0002
800–1600	0.002	<0.001	0.002	0.0004	0.0
1600–3200	0.0	0.0	0.0	0.0	0.0

same six choices of SUSY parameters as in Ref. [11]; we take $A_0 = 0$, $\tan\beta = 2$, $m_t = 170$ GeV, and (1) $m_0 = m_{1/2} = 100$ GeV, for which $m_{\tilde{g}} = 290$ GeV and $m_{\tilde{q}} = 270$ GeV, (2) $m_0 = 4m_{1/2} = 400$ GeV, for which $m_{\tilde{g}} = 310$ GeV and $m_{\tilde{q}} = 460$ GeV, (3) $m_0 = m_{1/2} = 300$ GeV, for which $m_{\tilde{g}} = 770$ GeV and $m_{\tilde{q}} = 720$ GeV, (4) $m_0 = 4m_{1/2} = 1200$ GeV, for which $m_{\tilde{g}} = 830$ GeV and $m_{\tilde{q}} = 1350$ GeV, (5) $m_0 = m_{1/2} = 600$ GeV, for which $m_{\tilde{g}} = 1400$ GeV and $m_{\tilde{q}} = 1300$ GeV, and (6) $m_0 = 4m_{1/2} = 2000$ GeV, for which $m_{\tilde{g}} = 1300$ GeV and $m_{\tilde{q}} = 2200$ GeV.

From Fig. 4 it is relatively obvious how E_T^c should be chosen to search for SUSY in the multilepton plus multijet channels: if gluinos are relatively light [cases (1) and (2)], $E_T^c \sim 100$–150 GeV suffices to obtain a large signal to background ratio and a large event rate in all the channels. For the cases with heavier gluinos and squarks [cases (3)–(6), a larger value of E_T^c is necessary, though it should not be chosen too large as to cut out all the signal. For instance, $E_T^c \sim 200$ GeV should yield an observable signal, with a signal to background ratio larger than unity in all but the OS-dilepton channel. The *maximal* reach may be anticipated to occur in the 1ℓ channel—for cases (5) and (6), with $E_T^c = 400$ GeV, we expect ~ 20–100 events (vs a background of just about three or four events) after a year of LHC operation at its ''low'' luminosity of 10 fb^{-1}/yr.

We next examine in detail each of the multilepton plus multijet topologies as a function of SUGRA parameters.

1. Single lepton events

We begin by showing, in the m_0-$m_{1/2}$ plane, cross section contours for the 1ℓ signal after the cuts discussed above for $A_0 = 0$ and (a) $\tan\beta = 2$, $\mu < 0$, (b) $\tan\beta = 2$, $\mu > 0$, (c) $\tan\beta = 10$, $\mu < 0$, and (d) $\tan\beta = 10$, $\mu > 0$ in Fig. 5. We have shown the results for $E_T^c = 100$ GeV (solid) for which the total SM background from Fig. 4 is ~ 1300 fb, and also for $E_T^c = 400$ GeV (dotted), for which the background is very tiny at about 0.5 fb. For an integrated luminosity of 10 fb^{-1}, the corresponding 5σ limits are 57 fb and 1.1 fb, respectively.

To obtain these contours (as well as the corresponding contours for the OS, SS, and 3ℓ signals discussed below), we have first computed the signal cross section for each point on a 100 GeV $\times$ 100 GeV lattice in the m_0-$m_{1/2}$ plane, for points which do not fall inside the excluded shaded re-

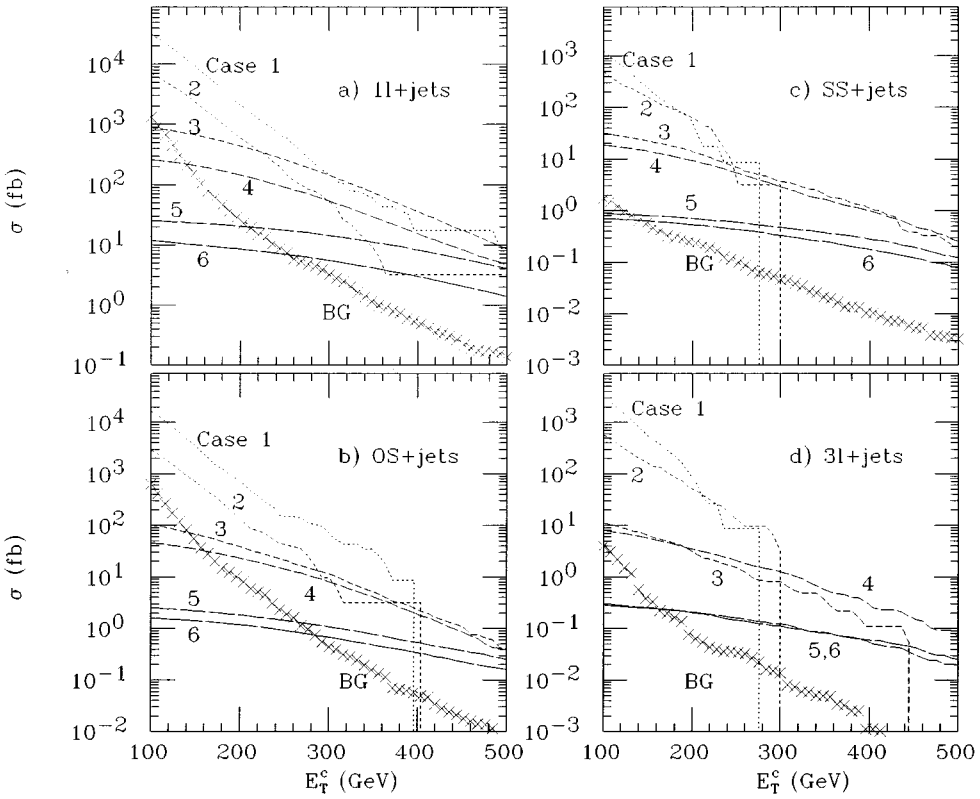

FIG. 4. SUSY signal cross sections for six SUSY cases listed in the text, and total SM background in fb, after cuts, as a function of the E_T^c parameter, for the same event topologies as in Fig. 3.

gions. The contours are then obtained via interpolation. We have cut off the contours near the boundaries of the shaded regions where the sampling is poorer and the interpolation not as reliable.

The curves shown are for cross sections of 1, 2, 4, 8, . . . fb (only every other solid curve is labeled) in each of these cases. We have also checked that, even for the very hard E_T^c cut, there are sufficiently many events in our simulation to yield reliable estimates of the cross sections: for the $E_T^c = 400$ GeV case, the efficiency for SUSY events to pass the cuts becomes very small unless sparticles are rather heavy, so that for moderate $m_{1/2}$ values, very lengthy com-

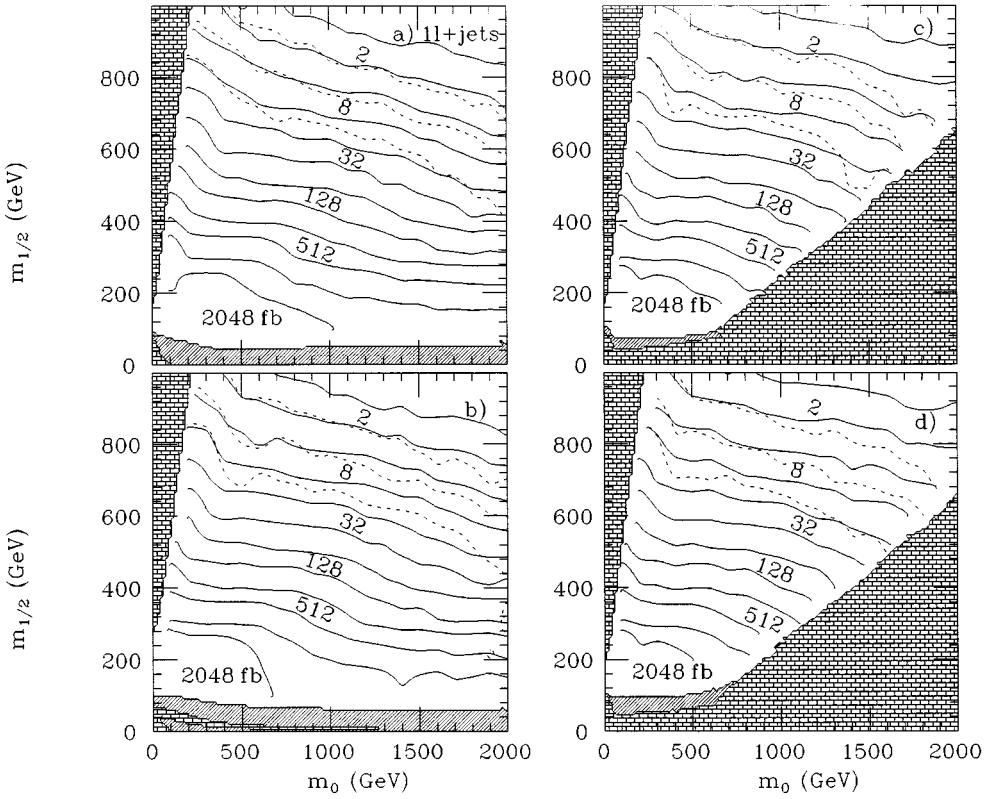

FIG. 5. Contours of cross section (in fb) after cuts described in the text for $1\not{\ell}+\text{jets}+\not{E}_T$ events. The solid contours have $E_T^c = 100$ GeV, while the dashed contours are for 1, 2, and 4 fb cross sections with $E_T^c = 400$ GeV, from which the maximum reach is derived. The frames are for the same SUGRA parameter choices as in Fig. 1.

puter runs would be necessary to compute the cross sections. For this reason, and because very hard cuts are necessary only for the largest gluino and squark masses, we have shown only the first three dotted curves, corresponding to cross sections after cuts of 1, 2, and 4 fb.

We see from Fig. 5 that with $E_T^c = 100$ GeV, the 5σ reach (the 64 fb contour is closest to the 57 fb 5σ limit) in the 1ℓ channel extends to $m_{1/2} \sim 600$ GeV for small values of m_0 (corresponding to $m_{\tilde{g}} \sim m_{\tilde{q}} \sim 1.5$ TeV), or to $m_{1/2} \sim 400$ GeV ($m_{\tilde{g}} \sim 1$ TeV) if squarks are heavy. Regions below this 5σ contour all have larger signal cross sections, so that we found no ''holes'' of nonobservability below the 5σ limit. Notice, however, that the signal to background ratio at the 5σ limit is just less than 5%: if we require this ratio to exceed 25%, the corresponding reach is between the 256 and 512 fb contours. To probe values of $m_{1/2} \gtrsim 250$–300 GeV, it is best to choose larger values of E_T^c to obtain a better statistical significance as well as a higher signal to background ratio. The maximal reach in the 1ℓ channel can be obtained by using a hard E_T^c cut which eliminates essentially all the background but still retains the signal at an observable level. The highest of the dotted contours (1 fb) is very close to the 5σ limit for $E_T^c = 400$ GeV; in this case, signal/background ~ 1, and $m_{1/2} \sim 700$ GeV (1000 GeV) can be probed in the large (small) m_0 region. This corresponds to a reach in $m_{\tilde{g}} \sim 1700$ GeV (2300 GeV). Thus, we note that *the reach in this channel appears to substantially exceed the corresponding reach [6,11] in the canonical multijet $\not{E}_T$ (no isolated lepton) channel.*

How well can one determine the SUSY parameters by studying the $1\ell + \text{jet} + \not{E}_T$ signal? Measurement of the total rate for such events would localize, within errors, a position along one of the total cross section contours of Fig. 5. These contours vary strongly with $m_{1/2}$, but less strongly with m_0. The cross sections are roughly the same in all the four frames. While this means that the 1ℓ signal rate yields no information about $\tan\beta$ or $\text{sgn}\mu$, it also means that a measurement — and calculation — of the cross section to within a factor of 2 would indeed tell us on which contour we are within about ± 50 GeV. While this does not accurately pin $m_{1/2}$ because the contours are not quite horizontal, one would still be able to obtain a reasonable estimate of $m_{1/2}$. The range of $m_{1/2}$ thus obtained can be checked for consistency with the gluino mass that might be extracted [11] from the $\not{E}_T$ channel: in fact, a similar measurement ought to be possible in the 1ℓ channel.

Determination of m_0 is more difficult and will probably require a simultaneous study of several signals and their distributions. We note, however, that for very small values of m_0, because of the enhancement of the leptonic decays of $\widetilde{W}_1$, and frequently also of $\widetilde{Z}_2$, the lepton plus multijet cross sections are large. In contrast, the 0ℓ plus multijet cross sections (for a fixed value of $m_{1/2}$) actually reduce [11] as $m_0 \to 0$ because of the lepton veto: thus, a measurement of the ratio of nonleptonic to multileptonic multijet cross sections could yield information on whether we are in the small m_0 region, particularly in the region where two body decays of $\widetilde{W}_1$ and/or $\widetilde{Z}_2$ into real sleptons are kinematically allowed (this region has been delineated in Fig. 15 below).

Next, we turn to an examination of the single lepton charge asymmetry, which could provide an additional handle on position in parameter space. Since LHC is a pp collider, there is a preponderance of valence u quarks in the initial scattering state, which can lead to a large proportion of $\tilde{u}$ squarks being produced in the final state if squarks are moderately heavy and gluinos not too light (otherwise, sea-parton annihilation may be the dominant source of sparticles). The $\tilde{u}$ squarks frequently decay to $\widetilde{W}_1^+$, and one is led to expect more ℓ^+s being produced than ℓ^-s. For large m_0 compared to $m_{1/2}$, $\tilde{g}\tilde{g}$ production should be dominant, which leads to equal production of ℓ^+ and ℓ^- in cascade decays. Likewise, as we already noted, if $m_{1/2}$ is small, then sparticle production at the LHC is dominated by gluon fusion and sea-quark annihilation, which also leads to equal ℓ^+ and ℓ^- production. In contrast, for larger values of $m_{1/2}$ and not too large m_0, the squark production via valence quarks can dominate, and lead to the lepton charge asymmetry. To illustrate this, we show in Fig. 6 the single lepton charge asymmetry

$$A_c = \frac{N(\ell^+) - N(\ell^-)}{N(\ell^+) + N(\ell^-)},$$

vs m_0, for (a) $m_{1/2} = 100$ GeV, using $E_T^c = 100$ GeV, (b) $m_{1/2} = 200$ GeV, using $E_T^c = 200$ GeV, (c) $m_{1/2} = 400$ GeV, using $E_T^c = 400$ GeV, and (d) $m_{1/2} = 500$ GeV, using $E_T^c = 400$ GeV. In all frames, $A_0 = 0$ and $\tan\beta = 2$. For frames (a)–(d), we take $\mu < 0$; frames (e)–(h) are the same except that $\mu > 0$. The horizontal dashed line is at $A_c = 0$. The rather small SM background (see Fig. 3) has not been included in these figures. We indeed see that for the small $m_{1/2}$ cases of frames (a) and (e), the asymmetry is consistent with zero (by choosing a larger E_T^c value, it may be possible to enhance the valence contribution and so obtain an asymmetry even in this case). As we move up in $m_{1/2}$ values, a significant positive charge asymmetry develops, especially for small values of m_0, reflecting the relative contribution of $\tilde{u}$ squarks vs $\tilde{d}$ squarks, or other squark flavors or gluinos. Knowledge of $m_{1/2}$ may thus be combined with the measurement of A_c to roughly localize m_0—we would at least learn whether $m_0 \lesssim m_{1/2}$ or whether $m_0 \gtrsim m_{1/2}$.

In order to explore other strategies for the determination of m_0, in Fig. 7 we have shown the mean jet multiplicity ($\langle n_j \rangle$) as a function of m_0 for the same eight cases (a)–(h) as in Fig. 6. We see that for a fixed value of $m_{1/2}$ (which can be determined from other considerations), $\langle n_j \rangle$ clearly increases with m_0. The underlying physics is exactly the same [11] as for the $\not{E}_T$ sample: for small m_0, squark production is a significant source of $\not{E}_T$ events, and because $\tilde{q}_R$ frequently directly decay via $\tilde{q}_R \to q\widetilde{Z}_1$, the mean jet multiplicity is reduced. The mean jet multiplicity is essentially independent of the sign of μ. We see, however, that it can increase by as much as a whole unit as m_0 varies between 100 GeV and 1 TeV. We also see that the precision with which m_0 can be determined depends on the values of other SUSY parameters. Finally, we note that although $\langle n_j \rangle$ changes only by about 30% as m_0 is varied over the whole range in the figure, this could mean a significant increase in the cross section for high multiplicity (say, $n_j \geq 4$ or 5) relative to $n_j = 2$, so that ratios of cross sections with different jet multiplicities could

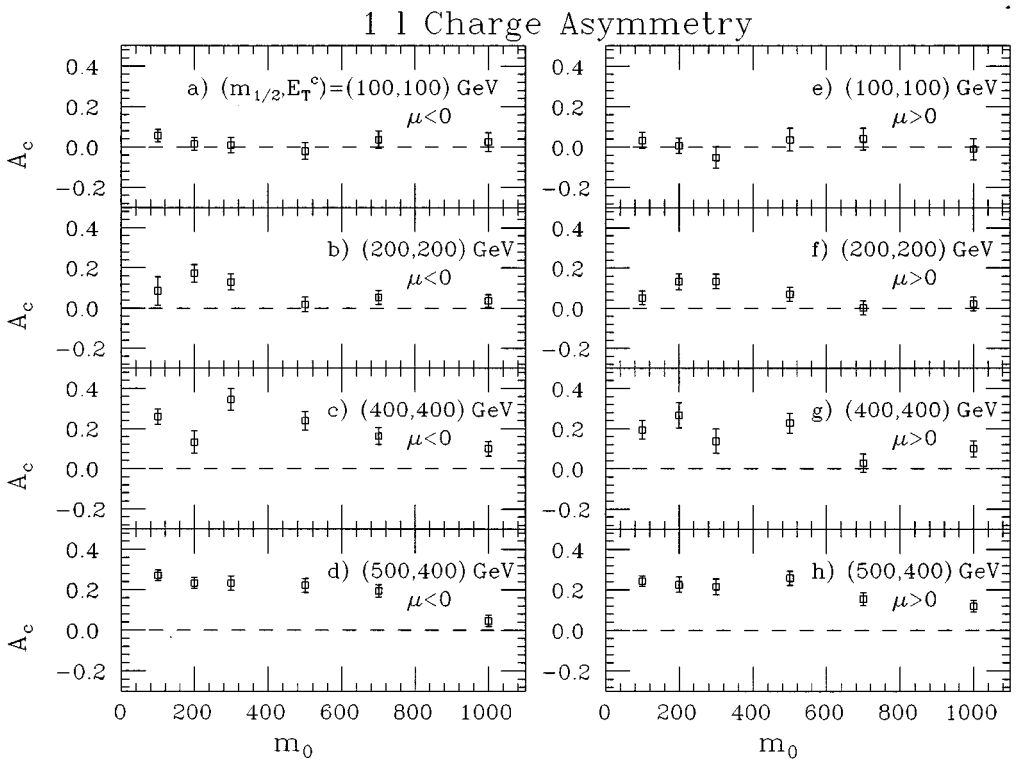

FIG. 6. Charge asymmetry A_c defined in the text of the isolated lepton in 1ℓ+jets+$\not{E}_T$ events. We have fixed $A_0=0$ and $\tan\beta=2$.

yield a more sensitive measure of m_0. Devising the optimal measure for localizing m_0 would require a detailed study beyond the scope of the present analysis.

The multiplicity of tagged B hadrons may also yield information about the underlying parameters. Towards this end, in Fig. 8 we have plotted the mean multiplicity ($\langle n_B\rangle$) of tagged B hadrons in the 1ℓ SUSY sample for the same cases as in Fig. 7, assuming that a B hadron with $p_T>20$ GeV and $|\eta_B|<2$ is tagged with an efficiency of 40%. We see from the figure that $\langle n_B\rangle$ varies between 0.2 and 1.3 over the parameter range shown. For the light gluinos, cases with $m_{1/2}=100$ GeV in frames (a) and (e), $\langle n_B\rangle$ is small and shows little variation with m_0, except around $m_0=200$ GeV where the decays $\tilde{g}\to b\tilde{b}$ dominate other squark decays. For

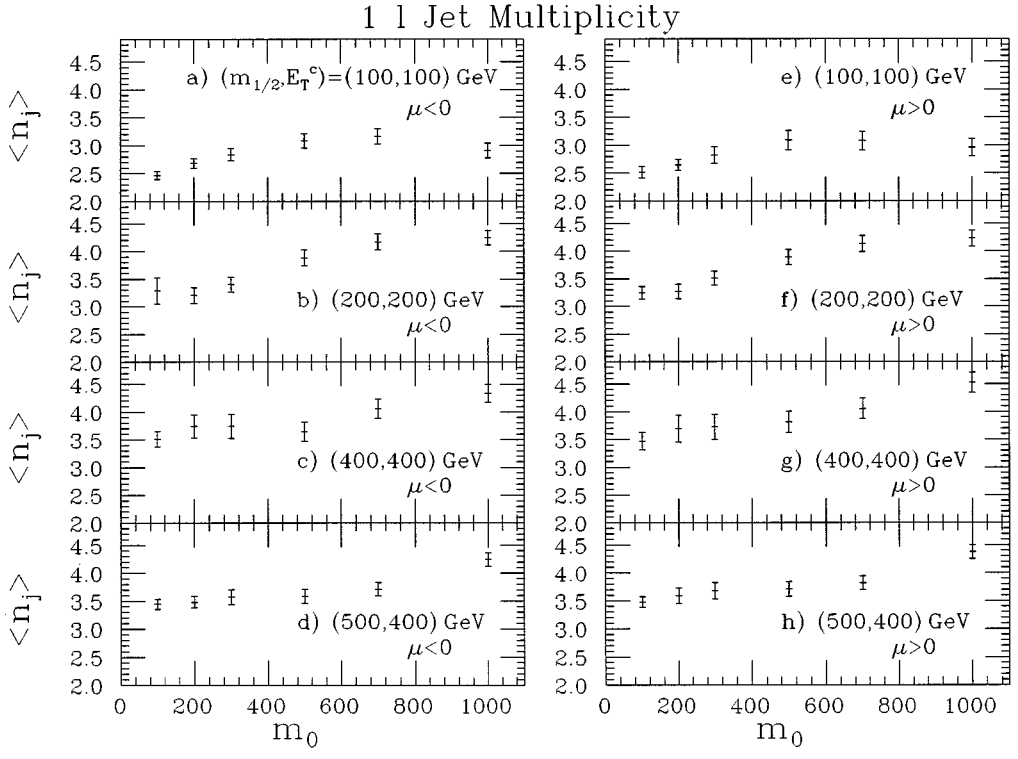

FIG. 7. The mean jet multiplicity $\langle n_j\rangle$ in 1ℓ+jets+$\not{E}_T$ events for the same cases as in Fig. 6. We have $A_0=0$ and $\tan\beta=2$.

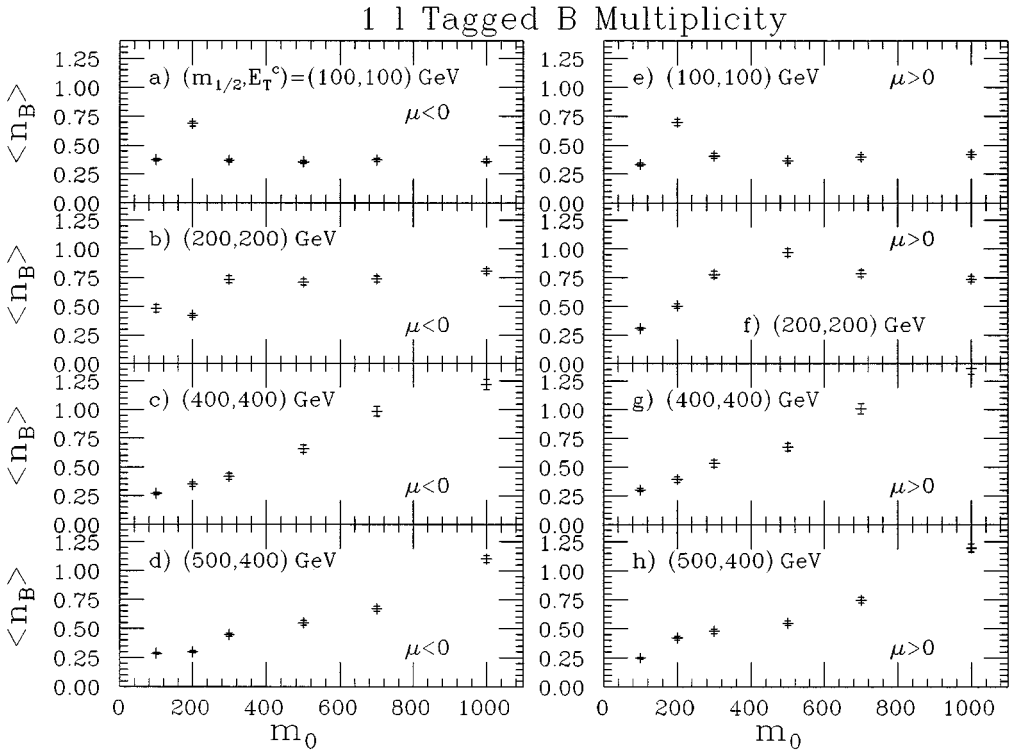

FIG. 8. The mean tagged b-hadron multiplicity $\langle n_B\rangle$ in 1ℓ+jets+$\not{E}_T$ events for the same cases as in Fig. 6. We have fixed $A_0=0$ and $\tan\beta=2$. The tagging requirements are described in the text.

large m_0, the gluino decays via the three-body modes, except that the decays to top quarks (which can potentially be enhanced) are kinematically suppressed. For heavier gluinos (i.e., larger values of $m_{1/2}$), there are two important differences. First, the spoiler decay $\widetilde{Z}_2\to\widetilde{Z}_1 H_\ell$, which is a source of B's, may be kinematically accessible: this leads to an increase in $\langle n_B\rangle$ which is roughly independent of m_0, except for the very small m_0 region where neutralino decays to sleptons are also accessible. Second, gluinos are heavy enough to decay to t quarks. Thus, when m_0 is very small, gluinos dominantly decay via $\widetilde{g}\to q\bar{q}$ into all flavors. As m_0 is increased, $\widetilde{g}\to\widetilde{t}_1 t$ or $\widetilde{b}_1 b$ may be kinematically allowed, while the $\widetilde{g}\to\widetilde{q}q$ modes are closed. For even larger values of m_0, three-body decays to third generation quarks can be enhanced because of propagator and large Yukawa coupling effects [40,41], leading to an increase in $\langle n_B\rangle$. Finally, we remark that $\langle n_B\rangle$ does not serve to discriminate between the two signs of μ. We caution the reader that $\langle n_B\rangle$ may potentially be sensitive to variations in A_0, since these may alter the masses and mixings of third generation sfermions. Thus, some care must be exercised when attempting to extract m_0 from a measurement of the B-hadron multiplicity.

2. Opposite sign dilepton events

Cross section contours for the OS dilepton signal are shown in Fig. 9 for the same cases as for the 1ℓ signal in Fig. 5. The solid lines are for $E_T^c=100$ GeV for which the SM background is 630 fb, while the dashed lines are for $E_T^c=200$ GeV for which the background is just 9 fb. As in Fig. 5 and in the subsequent figures, we show the dashed contours only for relatively large values of $m_{1/2}$ for which employing the larger E_T^c value is really essential. A striking feature of Fig. 9 is the sharp kink near $m_0\sim 400$ GeV where the contours change their slope. In cases (b)–(d), this is simply because of the opening up of the two-body decays of the chargino and $\widetilde{Z}_2$ into $\widetilde{\nu}$ and $\widetilde{\ell}_L$ [their branching fractions to $\widetilde{\ell}_R$ are strongly suppressed because $\widetilde{Z}_2$ ($\widetilde{W}_1$) has very small (zero) U(1) gaugino components]. In case (a), however, the kink in the 1 and 2 fb contours occurs at around $m_0=500$ GeV. We have checked that this is because $\widetilde{Z}_2$ and $\widetilde{W}_1$ leptonic *three-body* decays mediated by left-handed sleptons have significant branching fractions (few percent) even though the two-body decays $\widetilde{Z}_2\to Z\widetilde{Z}_1$ or $\widetilde{Z}_2\to H_\ell\widetilde{Z}_1$ and $\widetilde{W}_1\to W\widetilde{Z}_1$ are kinematically accessible: the resulting enhancement of the leptonic branching ratio, especially of $\widetilde{W}_1$, accounts for the kink being somewhat beyond the leptonic two-body decay region in case (a).

The 5σ observability level is at 40 fb for $E_T^c=100$ GeV and at 4.7 fb for $E_T^c=200$ GeV. We thus see from Fig. 9 that with $E_T^c=100$ GeV, the LHC should be able to observe a signal in this channel if $m_{1/2}\lesssim 300$–400 GeV (200–300 GeV if we also require $S/B>0.25$). The reach improves to $m_{1/2}=400$–500 GeV if the analysis is done using $E_T^c=200$ GeV. Notice that the reach is slightly larger in the $\tan\beta=10$ cases than those in the low $\tan\beta$ cases (a) and (b). This is because the branching fraction for the two-body $\widetilde{Z}_2\to Z\widetilde{Z}_1$ decay, which is very small for cases (a) and (b), is sizable when $\tan\beta$ is large. We have checked that the statistical significance of the signal is marginally improved with $E_T^c=300$ GeV, but the cross section is then just around 1 fb for $m_{1/2}=500$ GeV. In summary, with suitable cuts and 10 fb^{-1} of data, LHC experiments should be able to detect a signal in the OS-dilepton channel for $m_{1/2}$ up to 400–500 GeV, which corresponds to a gluino mass just beyond 1 TeV.

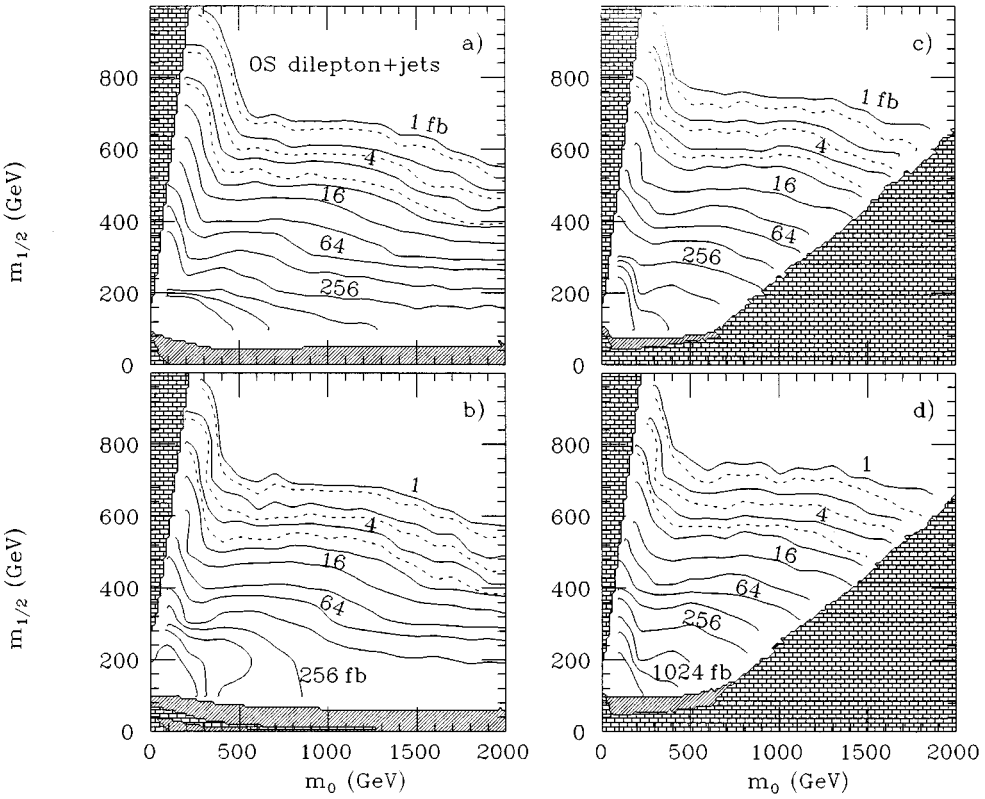

FIG. 9. Contours of cross section (in fb) after cuts for OS dilepton+jets+$\not{E}_T$ events. The solid contours have $E_T^c=100$ GeV, while the dashed contours are for 1, 2, and 4 fb cross sections with $E_T^c=200$ GeV, from which the maximum reach is derived. The frames are for the same SUGRA parameter choices as in Fig. 1.

If an OS dilepton signal is seen, one may again attempt to localize the position in parameter space via a measurement of the total OS dilepton cross section, which should place one along one of the contours in Fig. 9. Since the $\widetilde{Z}_2$ branching ratio into Z bosons depends on $\tan\beta$, the number of reconstructed $Z\to\ell\bar{\ell}$ events may offer some rough discrimination in that parameter if the spoiler modes are kinematically accessible. An idea of $m_{1/2}$ from the $\not{E}_T$ or 1ℓ channels together with the cross section in that channel would enable the determination of m_0 if it is small: for example, for $m_{1/2}=400$ GeV, the OS cross section rapidly varies from >128 fb (small m_0) down to 32 fb ($m_0\sim 500$ GeV), and then slowly decreases to $\lesssim 8$ fb. Ratios such as $\sigma(\mathrm{OS})/\sigma(1\ell)$ or $\sigma(\mathrm{OS})/\sigma(0\ell)$ would presumably be more accurately calculable than the absolute cross sections.

It was noted in Ref. [17] that the production of neutralinos in SUSY events can lead to a flavor asymmetry in the OS-dilepton event sample, which may allow further parameter space location. For instance, if OS dileptons are primarily coming from $\widetilde{Z}_2$ decay, then they should mainly be of same flavor, e.g., $e\bar{e}$ or $\mu\bar{\mu}$ pairs. If instead, OS dileptons come mainly from charginos or third generation quarks and squarks and their subsequent leptonic decays, then one would expect roughly equal abundance of $e\bar{\mu}$ and $\mu\bar{e}$ pairs as compared to same-flavor lepton pairs. We have plotted the OS dilepton flavor asymmetry:

$$A_F=\frac{N(e\bar{e})+N(\mu\bar{\mu})-N(e\bar{\mu})-N(\mu\bar{e})}{N(e\bar{e})+N(\mu\bar{\mu})+N(e\bar{\mu})+N(\mu\bar{e})}$$

in Fig. 10 for the same cases as in the previous figure. SM backgrounds are included in the figure. Points denoted by an x have an asymmetry $A_F<0.2$, consistent with no asymmetry in our simulation. Open boxes or diamonds have asymmetry $0.2<A_F<0.5$, while filled boxes or diamonds have $A_F>0.5$. For $m_{1/2}=100$ GeV, we took $E_T^c=100$ GeV, and we use the box symbols. For larger $m_{1/2}$, we took $E_T^c=200$ GeV to improve the signal/background, and we use the diamond symbols. We see in frame (a) that there is a large asymmetry for $m_{1/2}\lesssim 200$ GeV, and also for small m_0 values. In the former case, for small m_0, this is because of an enhanced branching fraction for $\widetilde{Z}_2\to\ell\bar{\ell}\widetilde{Z}_1$, while in the latter case it is, in part, because of the $\widetilde{Z}_2\to\ell\bar{\ell}_i$ two-body decays. In frame (*b*), the asymmetry disappears for small $m_{1/2}$ values because of interference effects driving the $\widetilde{Z}_2$ branching fraction to very small values [21,22]. The two frames for $\tan\beta=10$ continue to have significant flavor asymmetry even for $m_{1/2}$ as high as ~ 300 GeV because of the significant $\widetilde{Z}_2\to Z\widetilde{Z}_1$ branching fraction. Again, the significant asymmetry for small values of m_0 is because of real slepton decays of the neutralino. Note also that in some cases there is an observable asymmetry even when the leptonic branching fraction of $\widetilde{Z}_2$ is so small that the clean 3ℓ signal from $\widetilde{W}_1\widetilde{Z}_2$ production (discussed in Sec. IV) falls below the observable level. We thus see that an observation of a significant flavor asymmetry will localize us in the regions of the plane where at least one of m_0 or $m_{1/2}$ is not too large. Furthermore, if event rates indicate a large value of $m_{1/2}$, the observation of a flavor asymmetry would lead us to conclude that m_0 is rather small.

We also mention that we have checked that the jet multiplicity increases with m_0 for $m_{1/2}=200$ and 400 GeV, with other parameters fixed as in Fig. 7. We have also checked the $\langle n_B\rangle$ distributions which show a qualitatively similar trend as in the 1ℓ case shown above. Again the results are essentially

the same for the two signs of μ. We do not show these distributions for the sake of brevity.

3. Same sign dilepton events

The SS dilepton plus jets channel has long been known [37,38,3] to provide a clean signature for supersymmetry, and has been the subject of several studies [3,6,38,17,39] at the LHC. Within the MSSM framework, detailed simulations [6] have shown that, in this channel, the gluino reach extends to beyond 1 TeV. It is also known [17,39] that while gluino pair production with gluinos decaying via the chain $\tilde{g}\to\tilde{W}_1\to\ell$ is frequently considered to be the main source of these events, many other sources may be important, in particular, decays of gluinos to third generation fermions and also squark decays. We also stress that same-sign dilepton events do not necessarily originate via production of Majorana particles. For instance, the production of $\tilde{b}_1\tilde{b}_1$ pairs, where $\tilde{b}_1\to t\tilde{W}_1$, can also lead to SS dilepton plus multijet topologies. It is clear that a reliable computation of the SS-dilepton signal requires that all the decay chains as well as all possible production mechanisms be included, as is done in ISAJET.

The SS dilepton cross section is shown in Fig. 11 for the same values of SUGRA parameters as in Fig. 5 for $E_T^c=100$ GeV (solid contours) and $E_T^c=200$ GeV (dashed contours). As in Fig. 9 (and for essentially the same reasons), we see that the contours show a kink near the region where $\tilde{\ell}_L$ and $\tilde{\nu}$ masses approach $m_{\tilde{W}_1}\simeq m_{\tilde{Z}_2}$. The SM backgrounds to the signal are just 1.7 fb and 0.25 fb, respectively, yielding ''5σ'' limits of 2.1 fb and 0.8 fb. (For $E_T^c=200$ GeV, the Poisson probability of an expected background of 2.5 events fluctuating to 8 events is 4×10^{-3}, so that the 10-event level is perhaps a more reasonable estimate of the reach.) We see from Fig. 11 that even with $E_T^c=100$ GeV, the 5σ reach extends out to $m_{1/2}\sim400$–500 GeV, and up to 700 GeV in the small m_0 region, where squarks are relatively light and leptonic decays of $\tilde{W}_1$ and $\tilde{Z}_2$ are enhanced. The signal to background ratio exceeds unity. A higher value of E_T^c only gives a marginal increase in the reach. With the harder cut, the signal is small so that perhaps 20 fb^{-1} of integrated luminosity may be necessary in this case. As in Fig. 9, the cross sections are somewhat larger in the $\tan\beta=10$ cases as compared to the $\tan\beta=2$ cases. Finally, we note that although there are some fluctuations in our simulation for $m_{1/2}<200$ GeV, this signal should again be observable down to relatively low values of $m_{1/2}$.

Again, a measurement of the total cross section for SS dilepton events will place us along one of the contours in the m_0-$m_{1/2}$ plane. As before, a measurement of the ratio of the SS cross section to the 1ℓ cross section would be an indicator of the small m_0, large $m_{1/2}$ region. As in the OS dilepton case, the cross sections are somewhat larger for the high $\tan\beta$ cases. It has been pointed out [3] that a charge asymmetry may exist in any SS-dilepton signal detected at a pp collider; this observation has since been confirmed by more detailed simulations [6]. As for the asymmetry in the 1ℓ channel, the SS-dilepton charge asymmetry is again a reflection of the valence u and d quarks in the proton participating in the production mechanism. We show in Fig. 12 the charge asymmetry

$$A_c=\frac{N(\ell^+\ell^+)-N(\ell^-\ell^-)}{N(\ell^+\ell^+)+N(\ell^-\ell^-)},$$

as a function of m_0, for (a) $m_{1/2}=200$ GeV (with $E_T^c=100$

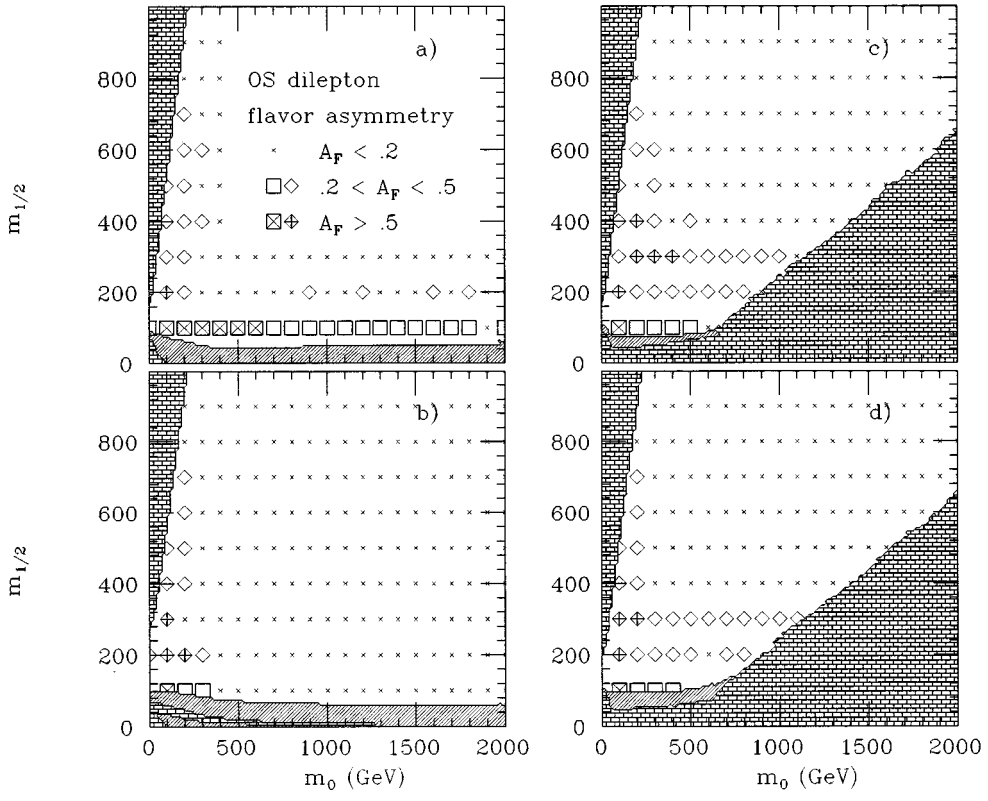

FIG. 10. Flavor asymmetry (A_F) defined in the text for the OS dilepton+jets+$\not{E}_T$ event sample for the same parameters as in Fig. 9. We use $E_T^c=200$ GeV (denoted by diamonds) except when $m_{1/2}=100$ GeV for which we use $E_T^c=100$ GeV (denoted by squares). The hollow (filled) symbols denote $0.2\leqslant A_F\leqslant0.5$ ($A_F\geqslant0.5$), while crosses show the points sampled for which $A_F<0.2$, which is consistent with zero in our simulation.

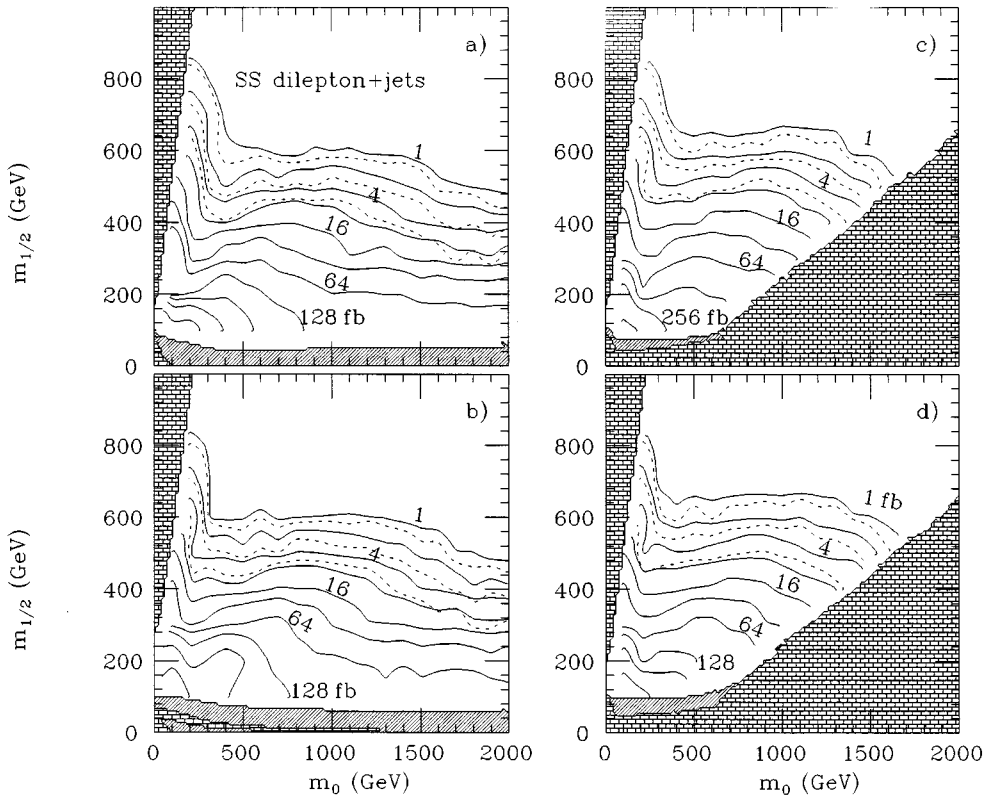

FIG. 11. Same as Fig. 9, except for SS dilepton+jets+$\not{E}_T$ events.

GeV), and (b) $m_{1/2}=400$ GeV (with $E_T^c=200$ GeV). We take $A_0=0$, $\tan\beta=2$, and $\mu<0$. Frames (c) and (d) are the same as (a) and (b), except for the sign of μ. It can be noted that for m_0 large, where $\tilde{g}\tilde{g}$ production is dominant, there is essentially no charge asymmetry. As m_0 decreases, and squarks become lighter, the asymmetry grows, reflecting the presence of $\tilde{u}$ squarks as a significant source of the event sample.

We have checked the dependence of the jet multiplicity in this sample on m_0 for the same cases as in Fig. 12. While we do see the anticipated trend for an increase of $\langle n_j\rangle$ with m_0, the extraction of m_0 appears more difficult than in the 1ℓ case, in part because of somewhat larger error bars in our simulation. We have also checked the $\langle n_B\rangle$ distributions for these same cases — they appear to be qualitatively similar to those for the 1ℓ and OS dilepton samples.

Finally, we have checked the sources of SS dilepton events for several points in parameter space to see how frequently these occur when each gluino decays via $\tilde{g}\to q\bar{q}\tilde{W}_1$ (where $q\neq t$) and $\tilde{W}_1$ decays leptonically since this chain has been suggested [38] as a way for extracting $m_{\tilde{g}}$. For small values of $m_0\simeq m_{1/2}$, this does not happen because gluinos

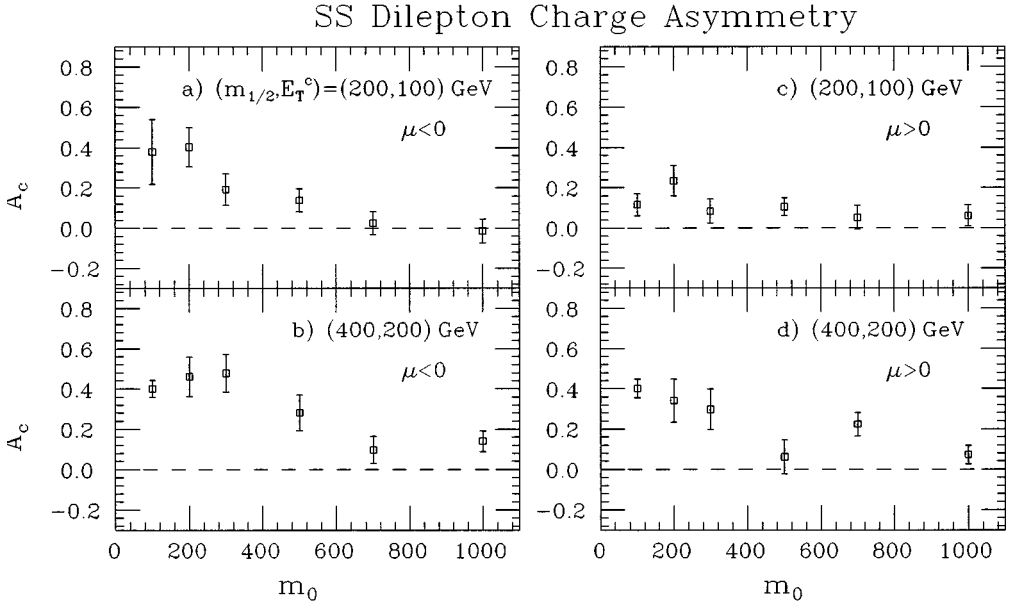

FIG. 12. Charge asymmetry A_c, defined in the text, of SS dileptons in $\ell^{\pm}\ell'^{\pm}$+jets+$\not{E}_T$ events. We have fixed $A_0=0$ and $\tan\beta=2$.

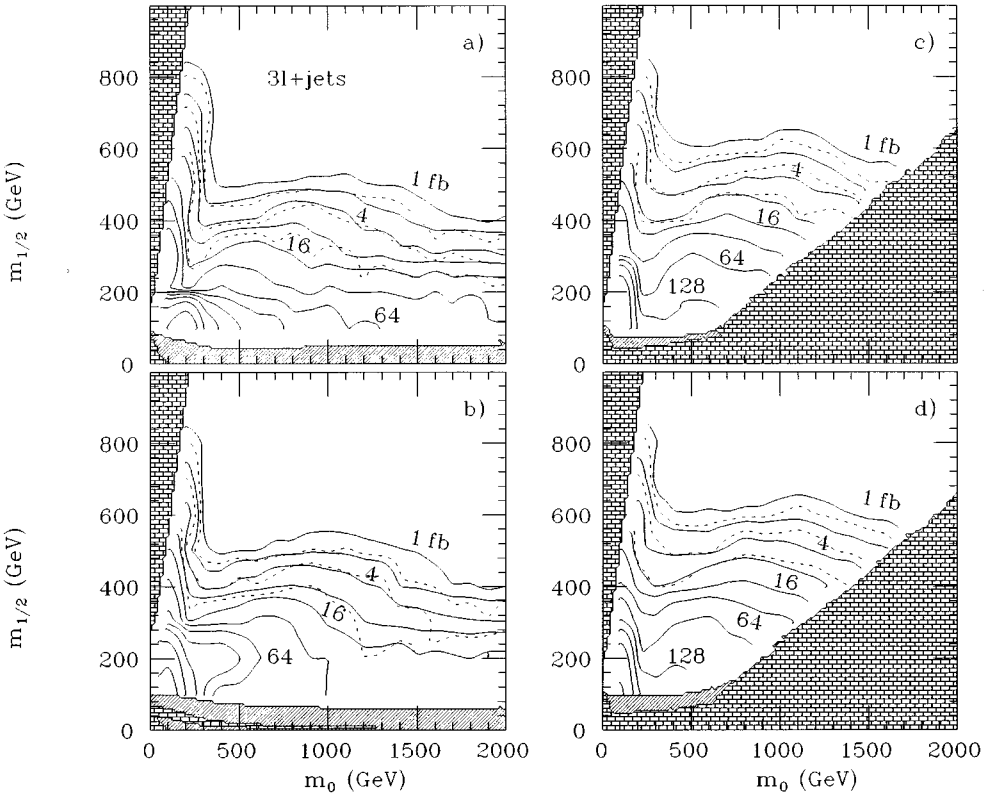

FIG. 13. Same as Fig. 9, except for $3\ell+\text{jets}+\not{E}_T$ events.

decay to real squarks. For $m_{1/2}=250$ GeV and $m_0=4m_{1/2}$, we have checked the sources in cases (a)–(c) of Fig. 11. We found that in these three cases, just 2/51, 3/36, and 0/48 events came from this particular cascade chain. Typically, in about half the SS dilepton event sample that passed the cuts, there was at least one t quark from the decay of the gluino (recall that decays to third generation may be enhanced), and greater than a third of the events had their origin in $\tilde{g}\tilde{q}_L$ or $\tilde{g}\tilde{q}_R$ production even though the squarks were somewhat heavier than gluinos. While these numbers do depend on the details of the cuts, they underscore the importance of simulating all possible production mechanisms and decay chains in order to make a realistic assessment of the feasibility of mass measurement in this channel.

4. Trilepton events

Finally, we show the cross section contours for $3\ell+\text{jets}+\not{E}_T$ events in Fig. 13, again for the same four cases (a)–(d); as before, $E_T^c=100$ GeV (solid) and 200 GeV (dashed). We note the following.

As expected, the cross sections are enhanced in the region where the two-body decays of $\tilde{W}_1$ and $\tilde{Z}_2$ to $\tilde{\ell}_L$ and $\tilde{\nu}$ are kinematically allowed.

The cross sections remain substantial even in the region of the plane where the spoiler decays of $\tilde{Z}_2$ (the boundaries of these regions are denoted by dotted lines in Fig. 2) become kinematically allowed. We thus conclude that while the cascade decay chains $\tilde{g}\to q\bar{q}\tilde{Z}_2\to q\bar{q}\ell\bar{\ell}\tilde{Z}_1$ or $q\tilde{}\to q\tilde{Z}_2\to q\ell\bar{\ell}\tilde{Z}_1$ are important sources of leptons in these events, there must be other sources operating as well. These include cascade decays of squarks and gluinos to charginos (which decay to W bosons) and to top quarks. We remind the reader that gluino decays to third generation quarks can frequently be enhanced [40,41,39] because $\tilde{t}_1$ and $\tilde{b}_1$ are frequently lighter than other squarks (so there is more phase space), because the third generation Yukawa couplings can be large and enhance such decays, and because Higgs bosons that are produced in the decay cascades decay either to third generation fermions, or to charginos and/or neutralinos (which have enhanced decays to third generation fermions).

For $m_{1/2}\gtrsim 250$ GeV (the boundary of the Z spoiler in Fig. 2), some of the trilepton sample (or the dilepton sample in Fig. 9) should consist of real $Z+\ell$ (real Z) events.

There are regions of parameter space [21,22] where the leptonic decays of $\tilde{Z}_2$, and hence the 3ℓ signal, are suppressed. This causes a dip in the cross sections of frames (c) and (d) around $(m_0,m_{1/2})\sim(300,200)$ GeV. It is instructive to compare this with the corresponding case for the clean trilepton signal from $\tilde{W}_1\tilde{Z}_2\to 3\ell$ discussed in the next section.

We find background cross sections of 4 fb and 0.07 fb, respectively, for the two choices of E_T^c. The 5σ level for E_T^c corresponds to a cross section of 3 fb, while the 5–10-event level might be a reasonable estimate for the reach with the larger value of E_T^c. We thus see that with $E_T^c=100$ GeV, the reach in the trilepton channel extends up to 350–500 GeV depending on the parameters, except of course in the small m_0 region where $m_{1/2}$ values as high as 700 GeV may be probed. Again, the reach is larger in the $\tan\beta=10$ cases. With $E_T^c=200$ GeV, the reach in $m_{1/2}$ increases by about 50 GeV. However, since the background is essentially negligible in this case, it may be possible to push the limits even

further with a larger data sample.

As with the other multilepton channels discussed earlier, there should be distinctive properties of the $3\ell+\text{jets}+\not{E}_T$ signal that allow some localization of where one is in parameter space. These include jet multiplicity, B multiplicity, and various p_T distributions. Also, there should again be a charge asymmetry, where we expect more $++-$ events than $+--$ events. We have also checked the variation of $\langle n_j \rangle$ with m_0. The distributions are somewhat flatter in this case as compared to the 1ℓ sample in Fig. 7. This is reasonable since for higher lepton multiplicity, the number of ''partonic jets'' must be correspondingly reduced. In contrast, the $\langle n_B \rangle$ distributions are qualitatively similar to the previous cases. We do not present these plots here for brevity.

5. A recapitulation of the LHC reach via multijet plus multilepton events

We have seen that, regardless of the model parameters, for $m_{\tilde{g}} \lesssim 1$ TeV ($m_{1/2} \lesssim 400$ GeV) there should be an observable SUSY signal in each of the 1ℓ, OS, SS, and 3ℓ channels if the SUGRA framework that we have adopted is a reasonable description of nature. In our previous study [11], we saw that there will also be a clearly observable signal in the jets$+\not{E}_T$ channel. Hence, in SUGRA, a wide variety of supersymmetric signals are expected to occur at the LHC. If gluinos are heavier than 1 TeV, the signals in the dilepton and trilepton channels may not be observable, although signals in the multijet$+\not{E}_T$ and 1ℓ channels may still be visible. The single lepton channel yields the maximal reach. Our computation shows that at the LHC, experiments will probe $m_{1/2}$ up to 600–700 GeV ($m_{\tilde{g}}$ up to 1500–1800 GeV) even if m_0 is very large; if m_0 is relatively small, it will be possible to search for gluinos heavier than 2 TeV [42].

Before closing this discussion, we should also mention that we have examined the 4ℓ channel [3]. We find that, with $E_T^c = 100$ GeV, these signals might be observable when $m_{1/2} \lesssim 300$ GeV for $\tan\beta = 2$ (or 500 GeV for $\tan\beta = 10$), the reach in this channel is always smaller than those in other channels. For this reason, and because there are rather few events in our simulation, we do not show these here. It should, however, be kept in mind that sparticle production can lead to these striking events at an observable level, especially if m_0 is small and $m_{1/2}$ not very large. Reducing or even eliminating the jet cuts could lead to larger signals in these event topologies without any large increase in the background (assuming that leptonically decaying Z bosons can be readily identified). We do not consider this any further in this study.

Up to now, we have fixed $A_0 = 0$ in our analysis. The cross sections should mainly depend on A_0 because of the variation of third generation squark masses. Instead of performing lengthy scans of the parameter space, we have illustrated the A_0 dependence of the cross section in Fig. 14 for six choices of A_0 and for $m_0 = 500$ GeV, $m_{1/2} = 160$ GeV, $\tan\beta = 2$, and $\mu > 0$. For $A_0 = 0$, 500, and 1000 GeV, gluinos decay via three-body modes into quarks plus various charginos and neutralinos. For larger, positive values of A_0, the decay patterns of $\tilde{t}_1$ are qualitatively similar to those for $A_0 = 1000$ GeV until A_0 exceeds ~ 1330 GeV, at which point $m^2_{\tilde{t}_R}$ becomes negative. For the three negative values of A_0 sampled, the top squark is so light that $\tilde{g} \to t\tilde{t}_1$ dominates the gluino decay channels (this is sensitive to other model parameters, including sgnμ). For $A_0 = -500$ and -900 GeV, the $\tilde{t}_1$ dominantly decays via $\tilde{t}_1 \to b\tilde{W}_1$, while for $A_0 = -950$ GeV, it is so light that only $\tilde{t}_1 \to c\tilde{Z}_1$ is allowed. For all A_0 values sampled, we see that the 1ℓ cross section is roughly constant to within a factor of ≤ 2. The dilepton cross sections show a somewhat larger variation, although this may not be sufficient, by itself, to determine A_0, since small changes in $m_{1/2}$ can cause similar variations. The maximum variation is seen in the 3ℓ cross section. The dilepton and trilepton cross sections are largest for cases with large negative A_0 values of which $\tilde{g} \to t\bar{\tilde{t}}_1$ and $\tilde{g} \to \bar{t}\bar{\tilde{t}}_1$ are the only two-body decays of the gluino. Since $\tilde{t}_1$ decays via $\tilde{t}_1 \to b\tilde{W}_1$, the increase in the leptonic cross sections (particularly for the 3ℓ channel) should not be surprising. The sharp drop in the cross sections at the most negative value of A_0 is because the chargino decay mode of the t squark (which is a source of leptons) becomes inaccessible, and $\tilde{t}_1 \to c\tilde{Z}_1$. In this case, $\tilde{g}\tilde{g}$ pairs (with $\tilde{g} \to t\tilde{t}_1$) can give rise to events with at most two hard, isolated leptons, and $\sigma(\text{SS}) \simeq \sigma(\text{OS})$. It may ultimately be possible from the ratios of multilepton to single lepton cross sections to pin down A_0, especially if it is close to the boundary of the excluded region where $m^2_{\tilde{t}_1}$ becomes negative. We have, however, seen that this ratio shows a similar trend in the small m_0 region where $\tilde{W}_1$ and $\tilde{Z}_2$ leptonic decays are enhanced. A measurement of $\langle n_B \rangle$ could serve to distinguish the two different origins of leptonic signals. We also note that, in principle, there could be parameter values for which $\tilde{g} \to b\tilde{b}_1$ might be the only allowed two-body gluino decay, in which case we would expect a reduction of the multilepton cross sections. More detailed study of the variation of the signals with A_0 are clearly necessary before definitive conclusions can be drawn.

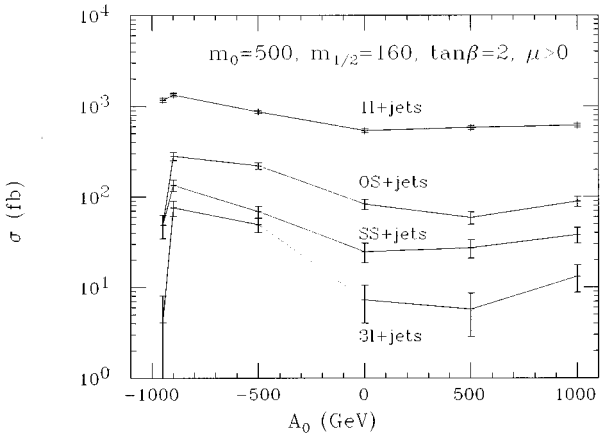

FIG. 14. An illustrative example showing the variation in cross section after cuts vs the SUGRA parameter A_0, for 1ℓ, SS, OS, and $3\ell+\text{jets}+E \not{a}p_T$ events. Other SUGRA parameters are listed in the figure. We take $E_T^c = 100$ GeV.

Our preliminary conclusions based on Fig. 14 are that (i) the multilepton cross sections examined above are less sensitive to variation in A_0 for lower lepton multiplicity, and (ii) except for the extreme cases where new channels for gluino

decays open up (these might be signaled by events with unusually high B-hadron multiplicity), even the multilepton cross sections are rather insensitive to A_0, and the choice $A_0=0$ that we have adopted yields representative values of these cross sections.

IV. CLEAN MULTILEPTON SIGNATURES FOR SUPERSYMMETRY

In the previous section, we focused on the study of multilepton events with at least two hard jets and substantial $\not{E}_T$. The cascade decays of gluinos and squarks were the main source of these jetty events. While the direct production of charginos, neutralinos, and sleptons can also lead to similar event topologies, these signals would be more difficult to pick out from SM backgrounds because of relatively lower total cross sections and softer $p_T(jet)$ and $\not{E}_T$ distributions. Moreover, there would be the additional issue of how to separate them from the corresponding signals from gluino and squark cascades for which the cross sections are considerably larger. Clean multilepton events, i.e., events without any jet activity, for which SM backgrounds are smaller, offer a more promising way of searching for chargino and neutralino [26,16] or slepton [24,25] signals at the LHC. We study the reach in SUGRA parameter space in these channels in this section.

Unlike in the previous section, where for each point in SUGRA parameter space we generated *all* SUSY subprocesses using ISAJET, here we focus on specific sets of reactions. This is because the majority of events generated contain gluinos and squarks which almost always yield hard jets, so that the efficiency for generating *clean* multilepton events is very small: the computer time that would be necessary to obtain an adequate sample of clean multilepton events would then make global scans of SUGRA space quite intractable. For sample points in the parameter space, we have checked how various SUSY channels contribute to the specific reactions that we are searching for.

A. Clean trilepton events from $\widetilde{W}_1\widetilde{Z}_2$ production

These signals have previously been studied [26,16] within the framework of the MSSM for parameter sets motivated by SUGRA models. In our previous study [16], we had fixed $\mu=-m_{\tilde{g}}$ and chosen $\tan\beta=2$ and $m_{\tilde{q}}=m_{\tilde{g}}+20$ GeV. We found that it was possible to find cuts which not only reduce SM backgrounds to negligible levels, but also isolate trileptons produced via $pp\to\widetilde{W}_1\widetilde{Z}_2+X\to\ell\nu\widetilde{Z}_1+\ell'\bar{\ell}'\widetilde{Z}_1+X$ from those produced by other SUSY reactions. These other SUSY processes typically contribute $\lesssim 10\%$ of the total trilepton signal, at least for the parameters where the signal was deemed to be observable. Here, we extend our previous study and explore the reach of the LHC for this signal within the SUGRA framework, and delineate the region of parameter space where the clean trilepton signal should be observable above SM backgrounds.

Exactly as in Ref. [16], we require (i) three isolated leptons, with $p_T(\ell_1,\ell_2)>20$ GeV, $p_T(\ell_3)>10$ GeV, (ii) a central jet veto, i.e., no jet with $p_T(\text{jet})\geq 25$ GeV within $|\eta_j|<3$, (iii) $\not{E}_T<100$ GeV, and (iv) $|m(\ell\bar{\ell})-M_Z|>8$ GeV for all combinations of OS leptons with the same flavor in the trilepton event.

Cuts (ii) and (iii) greatly reduce the backgrounds from the cascade decays of gluinos and squarks, while (iv) is designed to eliminate WZ events. After these cuts, tt remains the dominant background. It can be greatly reduced by further requiring (v) the two fastest leptons have the same sign of charge and the flavor of the slow lepton be the antiflavor of either of the two fast leptons.

This reduces the signal by 50% but essentially eliminates the top background, from which the two hardest leptons almost always come from the primary decays of the t quarks, and hence, have opposite signs of charge. To recover some of the rejected signal without a significant increase in the tt background, (vi) we retain events in which the two fastest leptons have opposite signs provided $p_T(\ell_3)>20$ GeV.

After cuts (i)–(iv) and either (v) or (vi), we find a SM background level [10] of 0.7 fb from WZ production where the gauge bosons decay into e, μ, or τ (which then decay leptonically), and 0.13 fb from tt production (for $m_t=170$ GeV), yielding a total SM background of 0.83 fb. This is somewhat larger than that in our earlier study [16] because of differences in parton distributions as well as calorimeter simulation. Assuming an integrated luminosity of 10 fb^{-1}, the minimum signal cross section for observability at the ''5σ level'' ($N_{\text{signal}}>5\sqrt{N_{\text{bkgds}}}$) works out to be 1.44 fb: the Poisson probability of an upward fluctuation of this amount is 2×10^{-5}. Notice that $N_{\text{signal}}/N_{\text{bkgd}}\geq 1.7$.

The region of the m_0–$m_{1/2}$ plane where the signal is observable at the 5σ (10σ) level is shown by hollow (solid) squares in Fig. 15 for $A_0=0$ and (a) $\tan\beta=2$, $\mu<0$, (b) $\tan\beta=2$, $\mu>0$, (c) $\tan\beta=10$, $\mu<0$, and (d) $\tan\beta=10$, $\mu>0$. For each parameter space point sampled, we require at least 25 events to pass the cuts in our simulation. The x's show the points that we have sampled but for which the signal falls below the 5σ level. Also shown in Fig. 15 are the boundaries of the region where the spoiler modes $\widetilde{Z}_2\to\widetilde{Z}_1H_\ell$ or $\widetilde{Z}_2\to\widetilde{Z}_1Z$, or two-body lepton-slepton decays of the neutralino become accessible. In cases (b)–(d), the boundary of the Higgs spoiler decay is not shown as it always lies above the boundary of the Z spoiler. Several features of this figure are worthy of mention.

In case (a), which corresponds most closely to the points sampled in Ref. [16], we see that the signal is observable at the 5σ level all the way up to the boundary of the spoiler modes, and for most of the region the significance is larger than 10σ.

There are regions of the m_0–$m_{1/2}$ plane in cases (b)–(d) where the chargino is at its current experimental bound from LEP, but where the trilepton signal fails to satisfy our 5σ criterion for observability. This was traced [36,21,22] directly to the leptonic branching fraction of $\widetilde{Z}_2$ which can drop by as much as two orders of magnitude because of interference effects between the slepton- and Z-mediated decay amplitudes. Thus a nonobservation of a signal in this channel will not allow us to infer a lower limit on either $m_{\widetilde{W}_1}$ or $m_{\widetilde{Z}_2}$. The regions of the parameter plane where there is an observable signal in this channel at the LHC are similar to the regions that the Tevatron operating at 10^{33} cm^{-2} s^{-1} could probe [21].

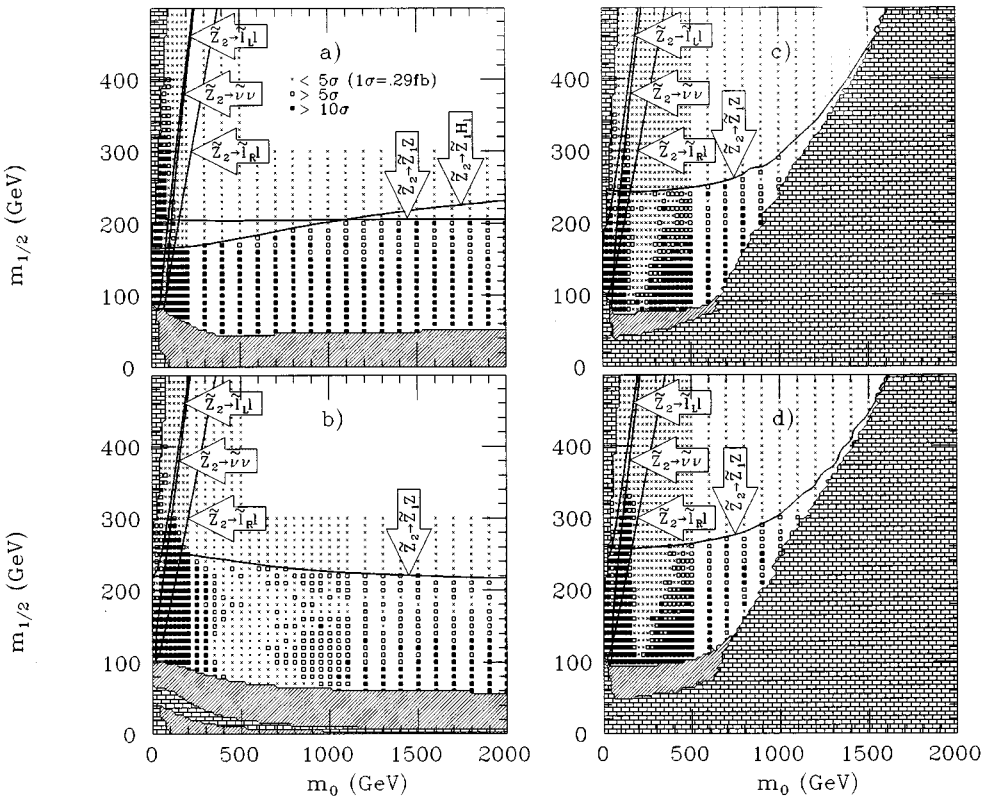

FIG. 15. Regions of the m_0 vs $m_{1/2}$ plane where clean (central-jet vetoed) isolated trilepton events are likely to be observable at the LHC, assuming 10 fb^{-1} of integrated luminosity. The frames are the same as in Fig. 1, except for the $m_{1/2}$ scale limits. The filled boxed correspond to a 10σ effect above background, open boxes to a 5σ effect, and crosses correspond to sampled points which were not observable with 10 fb^{-1}. In addition, the kinematic boundaries for various $\widetilde{Z}_2$ two-body decays are shown.

Except in the ''hole'' mentioned above, where there is no observable signal, the trilepton signal should be detectable all the way up to the limit of the spoilers. If sleptons are light enough so that $\widetilde{Z}_2 \to \widetilde{\ell}_{L,R}\ell$ are kinematically accessible (the small m_0 region of the plane), then these decays may dominate the spoiler decays. Then the branching fraction for leptonic decays of $\widetilde{Z}_2$ is very large, and the reach in the trilepton channel extends well beyond the boundary where the spoilers become accessible. Notice the small wedge between the contours labeled $\widetilde{Z}_2 \to \widetilde{\ell}_L\ell$ and $\widetilde{Z}_2 \to \widetilde{\nu}\nu$ where the signal drops because the invisible decay $\widetilde{Z}_2 \to \widetilde{\nu}\nu$ of the neutralino dominates.

We see that flipping the sign of μ makes a much larger difference in the $\tan\beta = 2$ cases (a) and (b) relative to the $\tan\beta = 10$ cases (c) and (d). This can be understood if we recall that it is always possible to choose μ and the gaugino masses to be positive by convention: then, the vacuum expectation values of the two Higgs fields can no longer be chosen to be always positive, and the physically relevant sign between μ and the gaugino masses appears as the sign of $\tan\beta$. Of course, for large values of $\tan\beta$, where one of the vacuum expectation values is essentially negligible, this sign is unimportant, explaining why the results in cases (c) and (d) appear so similar.

MSSM case studies of Ref. [16] suggest that the clean trilepton signal is relatively pure, and that the ''contamination'' from SUSY sources other than $\widetilde{W}_1\widetilde{Z}_2$ production is small. It should be kept in mind that in these studies we had fixed $\tan\beta = 2$ and chosen $\mu = -m_{\tilde{g}}$, so that the situation is roughly that in Fig. 15(a), where the signal exceeds 10σ over most of the plane. There are substantial regions of the parameter plane in cases (b)–(d) where the significance of the signal is between 5 and 10σ.

It has already been pointed out [16] that the isolation of the signal from $\widetilde{W}_1\widetilde{Z}_2$ production will allow a reliable determination of $m_{\tilde{Z}_2} - m_{\tilde{Z}_1}$, and perhaps also other combinations of chargino and neutralino masses.

B. Clean dilepton events from $\widetilde{W}_1\overline{\widetilde{W}}_1$ production

We have just seen that while charginos and neutralinos might be detectable over large regions of parameter space in the clean trilepton channel, there are parameter ranges for which the leptonic decays of $\widetilde{Z}_2$, and hence this signal, are strongly suppressed even if charginos are relatively light. We are thus led to examine whether OS dilepton signals from the reaction $pp \to \widetilde{W}_1\overline{\widetilde{W}}_1 + X \to \ell\overline{\nu\widetilde{Z}}_1 + \overline{\ell}\,\nu\widetilde{Z}_1 + X$ might be able to probe charginos in these regions, or to provide a new channel for confirmation of the existence of charginos detected in the trilepton channel; this was found to (at least partially) be the case for the 10^{33} cm^{-2} s^{-1} upgrade of the Fermilab Tevatron [21].

To search for events in this channel we have made the following cuts.

We focus on $e^{\pm}\mu^{\mp}$ events with $|p_T(\ell)| > 20$ GeV to eliminate large backgrounds from Drell-Yan production.

We veto events with any jet with $E_T > 25$ GeV within $|\eta| < 3$.

We require $30^0 < \Delta\phi_{e\mu} < 150^0$.

We require $\Delta\phi(\vec{p_T}(e\mu), \vec{\not{E}}_T) > 160^0$.

We require 40 GeV $< \not{E}_T < 100$ GeV (the upper limit on $\not{E}_T$ is to prevent other SUSY sources from contaminating the signal).

We have used ISAJET to compute SM backgrounds to the dilepton signal from $t\bar{t}$, WW, $\tau\bar{\tau}$, WZ, and ZZ productions. We find that our cuts efficiently suppress backgrounds from

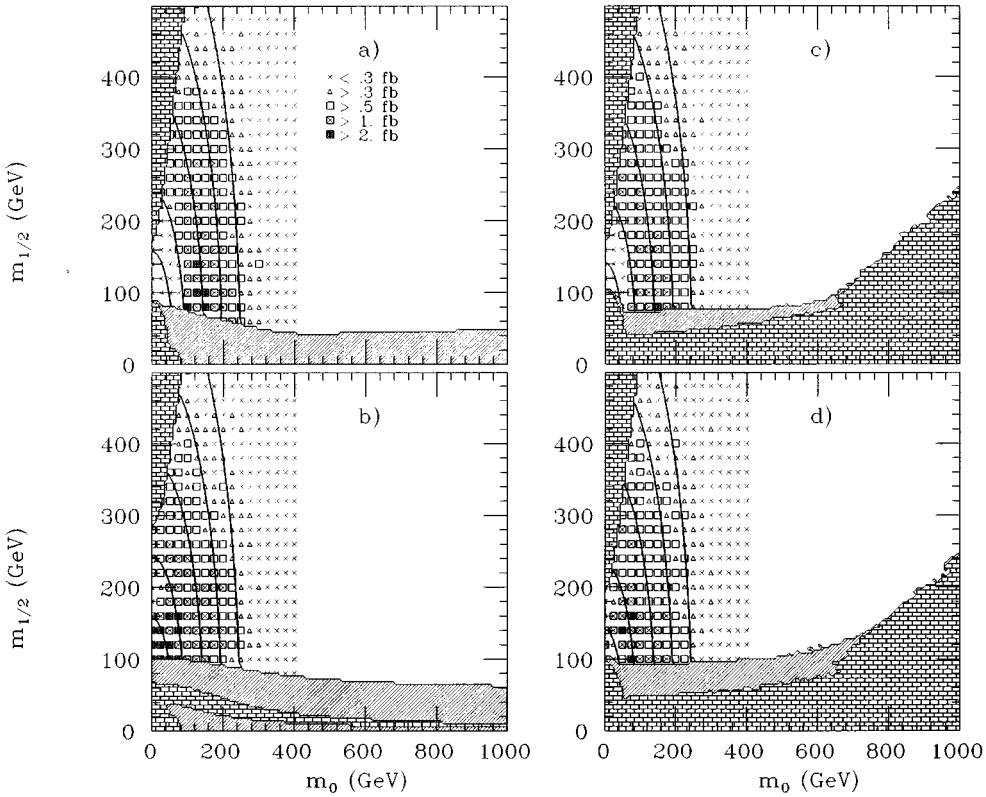

FIG. 16. Regions of the m_0 vs $m_{1/2}$ plane where clean (central-jet vetoed) isolated dilepton events (usually from slepton pair production) are likely to be visible using *hard slepton cuts* described in the text, assuming 10 fb^{-1} of integrated luminosity. The frames are the same as in Fig. 1, except for the scale limits. The various symbols correspond to the cross section levels after cuts listed on the figure. The estimated SM background level is 0.07 fb. The solid contours correspond to $m_{\tilde{\ell}_R}=70$, 100, 150, 200, and 250 GeV, increasing from the lower left.

all but WW events, for which the cut cross section is 136 fb [compared to the $\sigma(t\bar{t})=9.9$ fb and $\sigma(\tau\bar{\tau})=1$ fb]. For an integrated luminosity of 10 fb^{-1}, the 5σ level of observability corresponds to a signal cross section of 19 fb, although the signal/background ratio is small. We sampled points in the m_0–$m_{1/2}$ plane for the same cases as for the clean trilepton signal in the previous subsection. We found that except for a few points near $m_0=0$ in case (a) and an isolated point in case (c), the signal is below the 5σ level, and for most of the plane, even below the 3σ level. We conclude that, unlike at the Fermilab Tevatron upgrades, the dilepton signal from chargino pair production is unlikely to be observable above SM backgrounds.

C. Clean dilepton signals from slepton pair production

Charged sleptons and sneutrinos can be pair produced at the LHC in $q\bar{q}$ fusion processes via charged or neutral gauge boson exchange in the s channel. Their (cascade) decays can lead to event topologies with several leptons and jets in the final state. Previous studies [24,25] have shown that the clean, acollinear $e^+e^-+\not{E}_T$ and $\mu^+\mu^-+\not{E}_T$ channels offer the best hopes for the discovery of sleptons at the LHC. Our main purpose here is to delineate the region of the SUGRA parameter space where these signals might be observable at the LHC, and to check whether these can be distinguished from corresponding signals from chargino pair production.

To separate the signal from SM backgrounds, we require [25], (i) exactly two isolated same-flavor OS leptons, each with $|p_T(\ell)|>20$ GeV, (ii) $\not{E}_T>100$ GeV, (iii) a veto on central jets with $E_T>25$ GeV within $|\eta|<3$, and (iv) $\Delta\phi(\vec{p_T}(\ell\bar{\ell}),\vec{\not{E}}_T)>160^0$.

After cuts (i)–(iv), the dominant SM backgrounds to the SUSY signal come from $t\bar{t}$ (2.2 fb) and W^+W^- (2.9 fb), yielding a ''5σ observability level'' of 3.6 fb for a year of LHC operation at the design luminosity. The slepton cross section is, however, rather small and a higher reach is obtained with somewhat stiffer cuts to further reduce the background at modest cost to the signal. Hence, (v) for detection of heavy sleptons, we also require $|p_T(\ell)|>p_T^c$ and $\Delta\phi(\ell\bar{\ell})<\Delta\phi_c$, where p_T^c and $\Delta\phi_c$ can be adjusted appropriately. In our analysis, we fix $p_T^c=40$ GeV and $\Delta\phi_c=90^0$. Including cut (v), we find no event passes the cuts from our simulation of the WW sample (one-event level corresponds to $\sigma=0.0015$ fb in our simulation) while from $t\bar{t}$ events, we find a background cross section of 0.07 ± 0.006 fb. We thus expect <1 background event per LHC year with our ''hard'' cuts (i)–(v).

The region of the m_0–$m_{1/2}$ plane where slepton production should yield observable signals after these hard cuts is shown in Fig. 16, again for the same four cases as in previous figures. Since the SM background level is very small, we show contours of constant cross sections corresponding to the 3–5-event level per LHC year (triangles), 5–10-event level (hollow squares), 10–20-event level (squares with crosses), and >20-event level (filled squares). The crosses denote the sampled points for which the cross sections are smaller than 3 fb. We also show contours where $m_{\tilde{\ell}_R}=$ 70, 100, 150, 200, and 250 GeV. If we take the five-event level to give the optimistic reach, we see that the reach of the LHC extends to $m_{\tilde{\ell}_R}\sim250$ GeV, corresponding to $m_{\tilde{\ell}_L}$ and $m_{\tilde{\nu}}$ to just over 300 GeV for larger values of $m_{1/2}$. For a SM background expectation of 0.7 events, the Poisson probability of a

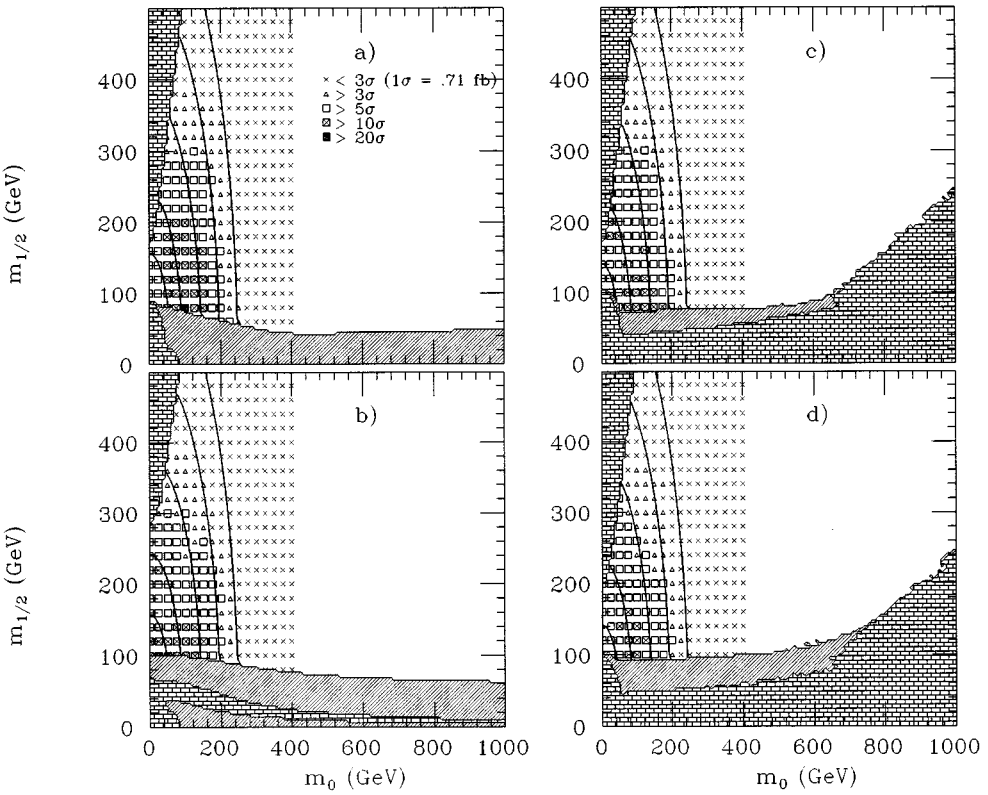

FIG. 17. Regions of the m_0 vs $m_{1/2}$ plane where clean (central-jet vetoed) isolated dilepton events (usually from slepton pair production) are likely to be visible *using soft slepton cuts*, assuming 10 fb^{-1} of integrated luminosity. The frames are the same as in Fig. 1, except for the scale limits. The various symbols correspond to the cross sections after cuts at the $<3\sigma$, $(3–5)\sigma$, $(5–10)\sigma$, $(10–20)\sigma$, and $>20\sigma$ levels. The solid contours correspond to $m_{\tilde{\ell}_R}=70$, 100, 150, 200, and 250 GeV, increasing from the lower left. Notice that with these cuts, the slepton signal is observable in the small m_0 region where it was not observable in Fig. 16.

fluctuation to the five- (ten-) event level is 8×10^{-4} (4×10^{-9}), so that a conservative estimate of the reach after a year of LHC operation is somewhere between 5 and 10 events.

More disturbing is the existence of the ''hole'' where the cross section falls below the five-event level for small values of m_0 and $m_{1/2}$ in cases (a) and (c). Notice that unless the energy of LEP 2 is upgraded so as to ensure the detectability of sleptons as heavy as 100 GeV, $\tilde{\ell}_R$ (and, of course, also $\tilde{\nu}$ and $\tilde{\ell}_L$) may evade detection at both LEP 2 as well as at the LHC. To understand why the hole is much larger for the $\mu<0$ cases, we have examined the differences in sparticle properties for $(m_0, m_{1/2})$ = (40 GeV, 140 GeV) in cases (a) and (b). For the negative μ case (a), $\tilde{W}_1$ and $\tilde{Z}_{1,2}$ are somewhat heavier than in case (b) so that the mass difference between $\tilde{\ell}_R$ and $\tilde{Z}_1$ is rather small (14 GeV, in our example). As a result, the efficiency particularly for $\tilde{\ell}_R\tilde{\ell}_R$ events to pass the *hard* $p_T(\ell)>p_T^c$ and $\not{E}_T$ cuts is reduced, leading to a drop in the cross section. For case (b) $m_{\tilde{\ell}_R}-m_{\tilde{Z}_1}=30$ GeV so that the daughter leptons are considerably harder. In addition, $\tilde{\ell}_L$ predominantly decays to $\tilde{W}_1$ and $\tilde{Z}_2$, and further, the leptonic branching fraction for $\tilde{W}_1$ is enhanced to 22%, while the neutralino decays via $\tilde{Z}_2\to\tilde{\ell}_R\ell$, so that hard leptons can come via several chains. This example also underscores the importance of incorporating the various cascade decays into the slepton analysis.

We have just seen that because of the hard cuts that we have used in Fig. 16, there are small regions of parameter space where sleptons with masses $\sim$80–120 GeV may evade detection both at LEP 2 and at the LHC. Because of the importance of this issue, we have redone our analysis using just cuts (i)–(iv) for which the SM background cross section is 5.1 fb. In Fig. 17 we show the regions of the m_0-$m_{1/2}$ plane where the significance of the signal $\sigma=N_{\text{signal}}/\sqrt{N_{\text{bkgd}}}$ is 3σ (triangles), 5σ (hollow squares), 10σ (squares with crosses), and 20σ (filled squares) for the same four cases as in Fig. 16. Indeed, we see that with the soft cuts, the slepton signal always exceeds the 5σ limit in the ''hole'' regions of Fig. 16, and further, that there is no window of masses where sleptons will escape detection both at LEP 2 and at the LHC. The maximal reach at the LHC is, of course, obtained using the *hard* cuts.

In order to check whether dilepton events from slepton pair production might be confused with corresponding events from chargino production, we have checked the origin of the events which satisfy our cuts for several cases: hard cuts, with $(m_0, m_{1/2})$= (210 GeV, 160 GeV), case (a) for which the slepton masses are 225–250 GeV and $m_{\tilde{W}_1}=155$ GeV, hard cuts with $(m_0, m_{1/2})$= (60 GeV, 160 GeV), case (b) for which the slepton masses are 92–135 GeV and $m_{\tilde{W}_1}=109$ GeV, and hard cuts with $(m_0, m_{1/2})$= (40 GeV, 140 GeV), case (b) for which the slepton masses are 75–115 GeV and $m_{\tilde{W}_1}=86$ GeV.

In all these cases, although we had generated all slepton (including sneutrino) as well as $\tilde{W}_1\tilde{W}_1$ events using ISAJET, we found that only slepton events in our sample of 40–60 events that pass our cuts; i.e., there was no event from direct chargino pair production in the sample. We did find events from cascade decays of sneutrino (produced in pairs or along with a charged slepton) as well as $\tilde{\tau}$s. To check whether chargino production contaminates the slepton sample with the soft cuts (i)–(iv) in Fig. 17, we have checked the sources for case (a) with $(m_0, m_{1/2})$ = (40 GeV, 140 GeV), for which the cross section is <0.3 fb after hard cuts, but where the

signal exceeds 5σ with soft cuts. We find that out of a total of about forty events that pass the cuts in our simulation, just six come from direct chargino production, with the charginos decaying via $\ell\tilde{\nu}_\ell$, ($\ell=e,\mu$). We thus conclude that a conclusive observation of a dilepton signal with the hard cuts will be unlikely to be confused with chargino pair production. There may, however, be some small chargino contamination of the signal with the soft cuts. In this case, the event sample should be large enough to provide other handles on chargino-slepton discrimination. For instance, if $m_{\tilde{e}_L}=m_{\tilde{\mu}_L}$, chargino production should lead to as many $e^\pm\mu^\mp$ events as $e^+e^-+\mu^+\mu^-$ events, whereas we would expect significantly more same-flavor events in the case of slepton pair production.

Finally, for the first two cases with the hard cuts above, as well as for the soft cut case we just discussed, we generated *all* SUSY subprocesses and ran them through the ''slepton cuts'' to see whether the ''slepton signal'' is contaminated by squark and gluino production, which occurs with a much larger cross section. This requires a simulation of a very large number of events since only a very tiny fraction of events passes the cuts. We examined the twenty events that satisfied the ''slepton cuts'' in each of these three cases: we found just one event from squark and gluino sources in one of the three event samples. However, in almost half the events for the $\mu<0$, hard cut and the soft cut cases, the leptons both originated from $\tilde{Z}_2$ decays in $\tilde{W}_1\tilde{Z}_2$ or $\tilde{Z}_2\tilde{Z}_2$ events (the leptons from the decay of a single $\tilde{Z}_2$ satisfy the $\Delta\phi$ cut more readily than those from $\tilde{W}_1\tilde{W}_1$ events). In the $\mu>0$, hard cuts case simulated, we have $m_{\tilde{\ell}_L}>m_{\tilde{W}_1}$, $m_{\tilde{Z}_2}>m_{\tilde{\ell}_R}$, so that $\tilde{Z}_2$ always decays via $\tilde{Z}_2\to\ell\tilde{\ell}_R$ into real sleptons: for this case, we found about 80% of the events had their origin in $\tilde{W}_1$ and $\tilde{Z}_2$ production. We thus conclude that while squark and gluino production is unlikely to contaminate the slepton sample, $\tilde{Z}_2$ decays from $\tilde{W}_1\tilde{Z}_2$ or $\tilde{Z}_2\tilde{Z}_2$ production can significantly contaminate the slepton signal (presumably $\tilde{W}_1\tilde{W}_1$ events frequently fail the $\Delta\phi$ cut, which fails to remove dileptons from $\tilde{Z}_2$ decays). However, these processes will themselves lead to characteristic signatures (the clean trilepton signature discussed above or even 4ℓ topologies) and would be detectable in their own right. We should also add that since these have not been included in Figs. 16 and 17, the actual cross sections may be somewhat larger than those shown in these figures.

Before drawing final conclusions regarding the detectability of sleptons at the LHC, we stress that we have assumed a 100% jet rejection efficiency for jets in the fiducial region. A real detector will, of course, have cracks and other dead regions. This is especially important here because the crucial cut [25] for the detectability of sleptons over the background from tt production is the central jet veto. In our previous analysis [25], we had shown that with the hard cuts, the tt background increases by about a factor of ~ 5 if instead this veto efficiency is 99%. Except to point out that it may be possible to reduce this detector-dependent background significantly by adjusting p_T^c and $\Delta\phi_c$, we will not discuss this any further. We thus conclude that if detectors have the capability to veto central jets with a high efficiency, it should be possible to probe $\tilde{\ell}_R$ and $\tilde{\mu}_R$ masses up to about 250 GeV at the LHC. The slepton signals are, however, very small so that perhaps 20–30 fb^{-1} of integrated luminosity may be necessary to confidently probe their existence.

Finally, we point out that in a recent paper [43], the cosmological relic density from neutralinos produced in the early Universe was evaluated for the same SUGRA model. In these calculations, it was found that a relic density of $\Omega h^2\sim 0.15$–0.4, which is favored by cosmological models with a critical density and a 2:1 mixture of cold and hot dark matter, would occur mainly if the slepton mass $m_{\tilde{\ell}_R}\sim 100$–$250$ GeV. Thus, failure to detect a slepton at LHC could place rather severe constraints on cosmological scenarios which ascribe the bulk of cold dark matter in the Universe to stable neutralinos.

V. COMPARISON OF RESULTS FROM THE VARIOUS CHANNELS

We have used ISAJET to map out the region of parameter space of the minimal SUGRA model with radiative breaking of electroweak symmetry where various n-jets plus m-leptons ($n\geq 2$, $m=1,2,3$) plus $\not{E}_T$ signals are observable above SM backgrounds at the LHC. These signals are dominantly expected to come mainly from gluinos and squark production followed by cascade decays. This paper is a continuation of our previous study [11] where we had focused on multijet plus $\not{E}_T$ events with an isolated lepton veto to reduce backgrounds from vector boson and top-quark production. We also examined the reach in the complementary clean dilepton and trilepton channels to investigate the detectability of the electroweak production of sleptons and charginos or neutralinos at the LHC.

Since the parameter space of the model is rather large, it is impractical to sample all regions of this space. One approach would be to generate random sets of model parameters (m_0, $m_{1/2}$, $\tan\beta$, A_0, $\mathrm{sgn}\mu$) and investigate various signals for the set of models thus obtained. This is the strategy used in Ref. [22] where the authors generated about $2K$ parameter sets in their exploration of the SUSY reach of the Fermilab Tevatron and its possible upgrade options. While this is indeed a viable strategy and may indeed have the advantage that it samples the parameter space ''more uniformly,'' it has some shortcomings. First, one has to choose how to sample each direction; e.g., should one randomly generate m_0 or $\ln m_0$, since the measure on parameter space is unknown. This is important because (for each sign of μ) just $1000^{1/4}=5.6$ points are generated on average along each of the four directions. Second, and more importantly in our view, while it is true that there may well be a fairer sampling of parameter space with this approach, it is difficult to relate the results to the underlying parameters of the theory. For these reasons, we have chosen to perform detailed scans in the m_0–$m_{1/2}$ plane (sparticle masses which dominantly determine the rates and distributions of the various signals are most sensitive to these parameters) for fixed values of $\tan\beta$ and A_0. We illustrate the results for a small ($\tan\beta=2$) and a medium ($\tan\beta=10$) value of $\tan\beta$. We do not consider larger values of $\tan\beta$ because the effects of bottom and tau Yukawa interactions, which could become important, have not yet been completely included in ISAJET. In most of our analysis, we fix $A_0=0$ (this does not mean

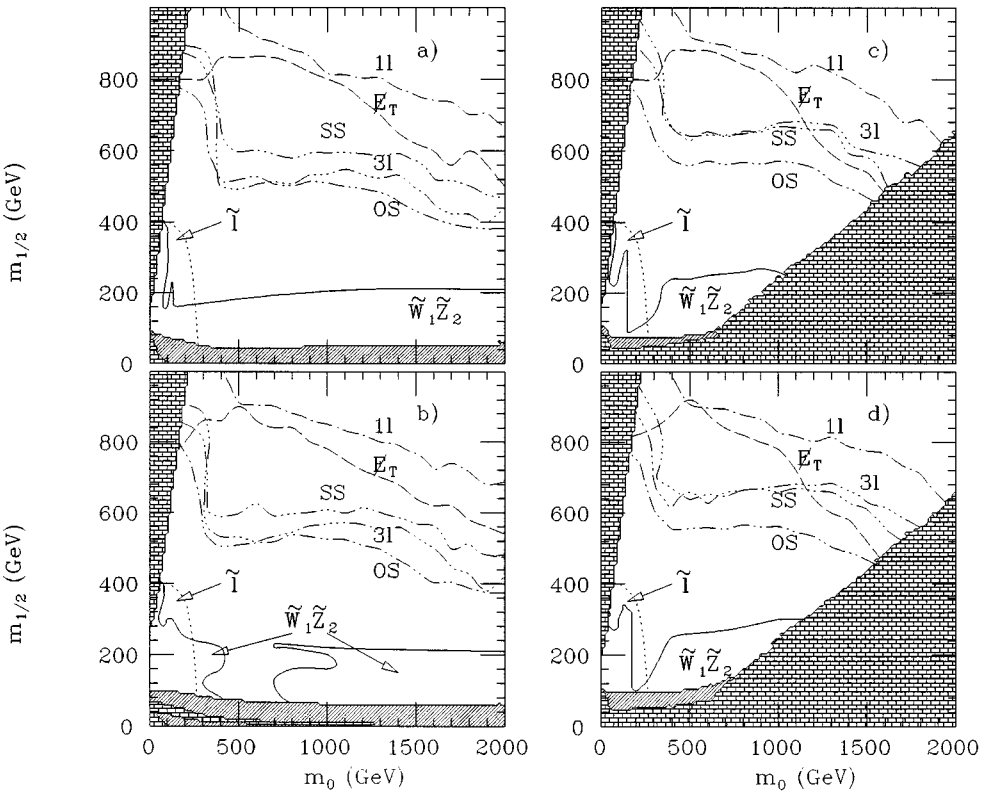

FIG. 18. A summary of the LHC reach (assuming 10 fb^{-1} of integrated luminosity) in the m_0 vs $m_{1/2}$ plane for the four cases of Fig. 1 via the various multilepton channels discussed in this paper. The dashed-dotted curves show the maximal LHC reach (obtained for some choice of E_T^c) for the 1ℓ, SS, OS, and 3ℓ+jets+$\not{E}_T$ signals. Also shown is the reach via the complementary clean dilepton (marked $\tilde{\not{l}}$) and clean trilepton (marked $\tilde{W}_1\tilde{Z}_2$) channels. The boundary of the parameter plane that can be probed via multijet+$\not{E}_T$ events (with no isolated lepton, denoted by $\not{E}_T$) as obtained in Ref. [11] shown for comparison as the dashed curve.

that the weak scale value of the A parameter vanishes) since our signals are moderately insensitive to this choice (see Fig. 14) except very close to the boundaries of the parameter space region where the correct pattern of electroweak symmetry breaking is not obtained.

The details of our calculation in the multijet channels may be found in Sec. III, while the clean multilepton signals are discussed in Sec. IV. Instead of repeating this discussion one more time, we have chosen to summarize the results for the LHC reach in the various channels in Fig. 18 for $A_0=0$ and (a) $\tan\beta=2$, $\mu<0$, (b) $\tan\beta=2$, $\mu>0$, (c) $\tan\beta=10$, $\mu<0$, and (d) $\tan\beta=10$, $\mu>0$. As before, the hatched (bricked) regions are excluded by experimental (theoretical) constraints. For a signal to be regarded as observable [44], we require that for an integrated luminosity of 10 fb^{-1} at the LHC, the event rates and numbers satisfy a statistical significance $\geq 5\sigma$, where $\sigma = N_{\rm signal}/\sqrt{N_{\rm bkgd}}$, $N_{\rm signal}/N_{\rm bkgd} \geq 0.2$, and $N_{\rm signal} \geq 5$.

In the region in Fig. 18 below the dashed line (labeled $\not{E}_T$), the 0 lepton plus $\not{E}_T$ signal should be observable beyond the 5σ level for an appropriate choice of the cut variable E_T^c defined in Sec. III as well as in paper I [11] from which these contours have been taken. The various dashed-dotted contours mark the boundaries of the region where the 1ℓ, same-sign (SS) dilepton, opposite-sign (OS) dilepton, and trilepton (3ℓ) plus multijet plus $\not{E}_T$ signals should be observable at the LHC, again for some value of $E_T^c \leq 200$ GeV (400 GeV in the case of the 1ℓ signal) as obtained from the analysis in Sec. III. The regions below the dotted line (labeled $\tilde{\not{l}}$) and solid line (labeled $\tilde{W}_1\tilde{Z}_2$) are where the clean dilepton and trilepton signals are observable as discussed in Sec. IV.

Several comments are worth noting:

At the LHC, it should be possible to detect gluinos as heavy as 1.5–1.8 TeV ($m_{\tilde{g}} \sim 2.3$ TeV if $m_{\tilde{q}} \simeq m_{\tilde{g}}$), corresponding to $m_{1/2} \lesssim 600$–700 GeV, after just one year of running at its lower design luminosity option of 10 fb^{-1}/y. This is considerably beyond [42] the bounds ($m_{1/2} \lesssim 400$ GeV) obtained from (admittedly subjective) fine-tuning arguments, and so should provide some safety margin for the detectability of SUSY at the LHC, at least within this minimal framework with conserved R parity. We also remark that we found no hole where these signals (or the multilepton signals, for that matter) might escape detection.

It is interesting that the maximal reach is obtained in the 1ℓ channel. This is because there are numerous sources of leptons in SUSY events so that a lepton veto significantly reduces the signal cross section. Our analysis using the E_T^c parameter shows that backgrounds from W boson and $t\bar{t}$ production (which lead to isolated leptons in the final states) can be controlled without vetoing events with leptons. It should thus be possible to combine the signals in the $\not{E}_T$ and 1ℓ channels to obtain a somewhat larger reach.

If squarks and gluinos are lighter than 1 TeV, several other signals should be observable above SM backgrounds if a signal in the $\not{E}_T$ or 1ℓ channels is to be attributed to sparticle production. Although our conclusion, strictly speaking, has been obtained in the rather constrained SUGRA framework, including constraints from radiative electroweak symmetry breaking (these essentially fix $|\mu|$), previous analyses [3] suggest that this will be true even if constraints from electroweak symmetry breaking are relaxed [45]. We also note that a portion of the multileptonic signals arise from leptonically decaying Z bosons. This is the reason why the reach in multilepton channels is slightly larger in the $\tan\beta=10$ cases (c) and (d) in Fig. 18. The real Z boson

signals are sensitive to the value of μ [3], and hence, to the radiative symmetry-breaking constraint.

While it appears that only a rather small subset of the parameter plane can be probed via the clean leptonic channels, the observation of these signals is important because it leads to direct detection of $\widetilde{W}_1$, $\widetilde{Z}_2$ (this sparticle may be hard to detect even at the NLC), and the sleptons. Moreover, it has been shown [16] that it is possible to isolate $\widetilde{W}_1\widetilde{Z}_2\to 3\ell$ events from SM backgrounds as well as from other SUSY sources. This allows for a reliable determination of $m_{\widetilde{Z}_2}-m_{\widetilde{Z}_1}$, and perhaps, other combinations of chargino and neutralino masses. We stress that the nonobservation of a trilepton signal at the LHC will not lead to a bound on the chargino or neutralino mass because of parameter space regions where the leptonic decays of $\widetilde{Z}_2$ are strongly suppressed. It is, however, interesting to note that even in these regions, the multijet plus 3ℓ signals are observable, implying that there are significant other sources of leptonic events (notably, third generation fermions and sfermions).

At the LHC, it should be possible to detect sleptons with masses up to 250 GeV (300 GeV for $\widetilde{\ell}_L$) in the clean OS dilepton channel. We have also shown that sleptons as light as 80 GeV ought to be detectable at the LHC using the ''soft cuts'' discussed in Sec. IV. Thus, there is no window where sleptons might escape detection, both at LEP 2 and at the LHC. Furthermore, the LHC is sensitive to the most favored range of slepton masses expected from calculations of the dark matter neutralino relic density ($m_{\widetilde{\ell}_R}\sim 100$–$250$ GeV) [43].

Aside from the question of the detection of SUSY, it is interesting to ask whether it is possible to devise tests of the various assumptions underlying the minimal SUGRA framework that we have adopted for our analysis. Tests that work well at an electron-positron collider [9,8] do not appear to be feasible at the LHC, partly because the initial state of the colliding partons is not known, and partly because of the messy interaction environment at the LHC. Alternatively, we may ask whether it is possible to use the multitude of observables that should be accessible at the LHC to determine the underlying parameters of the model. This is clearly a complex task since the directly observable quantities, such as cross sections in various channels, depend on various masses and mixing angles which have to be unraveled in order to get at the underlying parameters.

In this paper, we have made a first attempt to understand how it might be possible to use the LHC data to get at m_0 and $m_{1/2}$. We have little to say at present about the determination of $\tan\beta$, A_0, or $\mathrm{sgn}\mu$.

(1) If $m_{1/2}\lesssim 300$ GeV (so that gluinos are lighter than about 700–800 GeV), we had shown in paper I that it should be possible to measure $m_{\tilde{g}}$ to 15–25% by requiring hemispheric separation of events in the $\not{E}_T$ channel. Presumably, the same strategy can also be used in the 1ℓ channel. The value of $m_{\tilde{g}}$ can be directly related to $m_{1/2}$ [aside from the (usually small) corrections because of differences between the running and pole gluino masses].

(2) If the trilepton signal from $\widetilde{W}_1\widetilde{Z}_2$ production is observed at a substantial rate, it would be possible to check whether the value of $m_{\widetilde{Z}_2}-m_{\widetilde{Z}_1}$ is in agreement with the expectation from the gluino mass, assuming that $|\mu|$ is large and the unification condition for gaugino masses is valid. If the gluino and neutralino masses are not in accord with this expectation, we would probably conclude that $|\mu|$ is not large which would imply that we are somewhat close in parameter space to the boundary of the bricked region where the correct pattern of electroweak symmetry breaking is not obtained. The alternative would be that the gaugino mass unification condition is invalid.

(3) If the various multijet signals are observed at rates compatible with gluino masses corresponding to $m_{1/2}\leqslant 200$ GeV, but no clean trilepton signal is seen, we would probably infer that we are in one of the ''hole'' regions where the leptonic decays of $\widetilde{Z}_2$ are strongly suppressed. This would imply that m_0, and hence squarks and sleptons, cannot be too heavy (although there would be no guarantee that sleptons would be light enough to be observable).

(4) If a signal is observed in the OS dilepton channel with the ''slepton cuts'' of Sec. IV, we would place ourselves in the bottom left corner below the dotted line in the m_0-$m_{1/2}$ plane. In this case the multijet topologies from gluino and squark production *must* be seen. Otherwise, the assumptions of universal sfermion and/or gaugino mass at the ultrahigh scale, which imply $m_{\tilde{q}}^2=m_{\tilde{\ell}}^2+(0.7$–$0.8)m_{\tilde{g}}^2$, could not be valid.

It is possible that gluinos are rather heavy so that neither the $\widetilde{W}_1\widetilde{Z}_2$ nor the slepton signals are accessible. The determination of parameters is more difficult in this case. We have shown in Sec. III that the cross sections for multijet plus lepton signals will place us on one of the contours in Figs. 5, 9, 11, or 13. Because the multilepton contours are roughly horizontal (except in the $m_0\leqslant 400$–500 GeV region, to which we will come back to), it should be possible to get a rough idea of $m_{1/2}$ [roughly within $\pm(50$–$100)$ GeV] and hence, of $m_{\tilde{g}}$. It should also be possible to decide whether m_0 is small ($\lesssim 300$–400 GeV) or rather large, with a degree of confidence by studying the ratio of $\sigma(0\ell+\mathrm{jets})/\sigma(n\ell+\mathrm{jets})$ for $n=1$–3. For small values of m_0 and somewhat large values of $m_{1/2}$, the leptonic decays of charginos and neutralinos, and hence the multilepton signals, are enhanced. For the same reason, the $0\ell+$jets signal (because of the lepton veto) is reduced, as can be seen by the down turn of the corresponding contour in Fig. 18. This could be confirmed by a measurement of the flavor asymmetry in the OS dilepton sample (see Fig. 10). If gluinos are heavy, and $m_0\geqslant 500$ GeV, the determination of m_0 may be more difficult. Possible handles are the charge asymmetry in the 1ℓ and SS event samples (the asymmetry reduces with m_0) or the jet and B multiplicities in the 0, 1, and 2 lepton multijet samples (the multiplicity is larger for larger values of m_0). Clearly, detailed case studies beyond the scope of this analysis would be required to determine how well these model parameters can be determined.

We have not found any strategy for the determination of $\tan\beta$, A_0, or $\mathrm{sgn}\mu$. A qualitative idea of whether $\tan\beta$ is small (close to unity) or large might be obtained by looking for multijet events with real Z bosons: these are more abundant for larger values of $\tan\beta$. The observation of the Higgs boson and a measurement of its mass (perhaps in the $\gamma\gamma$ channel) may also provide a handle on this parameter: since $m_{H_l}=0$ at tree level if $\tan\beta=1$, the lightest Higgs boson

tends to be lighter when $\tan\beta$ is close to unity. The parameter A_0 mainly affects the third generation. Variations in A_0 can alter significantly the dominant gluino decay channels, so that rates in dilepton and, especially, trilepton plus multijet channels can have significant dependence on this parameter. The multiplicity of central B hadrons in SUSY events should also be sensitive to A_0. We have, however, not studied this aspect of parameter space in enough detail to draw any clear conclusions on A_0.

It may well be that all the parameters will ultimately be extracted by a global fit to all the data. The success of such a fit would certainly be nontrivial since the complete set of observations would need to be fitted by just four parameters (plus a sign). If an adequate fit is not possible, the assumptions underlying the model would need reexamination.

To sum up, if supersymmetry is the new physics that ameliorates the fine-tuning problem of the SM, it appears almost certain that there will be a multitude of new physics signals at the LHC. Although our analysis has been performed within the framework of the R-parity-conserving minimal SUGRA model, we do not expect the results to be qualitatively altered because of minor modifications of the model, as long as R parity is conserved. The maximal reach is obtained in the single lepton channel and it appears that gluinos as heavy as 1.5–1.8 TeV (2.3 TeV if squarks are degenerate with gluinos) ought to be detectable at the LHC with just 10 fb^{-1} of data. It should also be possible, in at least some cases, to identify the sparticle origins of various signals. We have also made a preliminary exploration to see how one might attempt to localize the underlying SUGRA model parameters, given that these SUSY signals are seen at the LHC. While this may well be easier at e^+e^- colliders (with sufficient center-of-mass energy), it is certainly worthwhile to think about what might be possible in experiments at the LHC, where construction has already been approved. We have argued that it might be possible to extract $m_{1/2}$ and, to some extent, also m_0 via a simultaneous study of several signals. Other parameters appear even more difficult to obtain, but this study should only be regarded as a first attempt in this direction.

ACKNOWLEDGMENTS

One of us (X.T.) is grateful to the High Energy Physics Group at Florida State University for their generous hospitality while this work was being carried out. In addition, C.H.C. thanks the Davis Institute for High Energy Physics. This research was supported in part by the U. S. Department of Energy under Contract Nos. DE-FG05-87ER40319, DE-FG03-91ER40674, DE-AC02-76CH00016, and DE-FG-03-94ER40833.

[1] For a review of the minimal model and SUSY phenomenology, see H. P. Nilles, Phys. Rep. **110**, 1 (1984); H. Haber and G. Kane, *ibid.* **117**, 75 (1985); R. Arnowitt and P. Nath, in *Particles and Fields*, Proceedings of the VII J. A. Swieca Summer School, Sao Paulo, Brazil, 1993, edited by O. Eboli and V. Rivelles (World Scientific, Singapore, 1994); V. Barger and R. J. N. Phillips, in *Recent Advances in the Superworld*, Proceedings of the International Workshop, Woodlands, Texas, 1993, edited by J. Lopez and D. Nanopoulos (World Scientific, Singapore, 1994); *Properties of SUSY Particles*, edited by L. Cifarelli and V. Khoze (World Scientific, Singapore, 1993); X. Tata, Lectures presented at TASI95, University of Colorado at Boulder, Hawaii Report No. UH-511-833-95, 1995 (unpublished).

[2] H. Baer *et. al.*, to appear in *Electroweak Symmetry Breaking and New Physics at the TeV Scale*, edited by T. Barklow, S. Dawson, H . Haber, and J. Seigrist (World Scientific, Singapore, 1995).

[3] H. Baer, X. Tata, and J. Woodside, Phys. Rev. D **45**, 142 (1992); H. Baer, M. Bisset, X. Tata, and J. Woodside, Phys. Rev. D **46**, 303 (1992); C. Albajar *et al.*, in *Proceedings of the ECFA Large Hadron Collider Workshop*, Aachen, Germany, 1990, edited by G. Jarlskog and D. Rein (CERN Report No. 90-10, Geniva, Switzerland, 1990); F. Pauss, *ibid.*

[4] The Solenoidal Detector Collaboration Technical Design Report, No. SDC92-201, 1992 (unpublished).

[5] GEM Collaboration, Technical Design Report, No. GEM-TN-93-262, 1993 (unpublished).

[6] ATLAS Collaboration, Technical Proposal, No. CERN/LHCC 94-43, 1994 (unpublished).

[7] Our use of the terms MSSM and SUGRA are as defined in Ref. [11].

[8] JLC-1, KEK Report No. 92-16, 1992 (unpublished).

[9] T. Tsukamoto, K. Fujii, H. Murayama, M. Yamaguchi, and Y. Okada, Phys. Rev. D **51**, 3153 (1995).

[10] C-H. Chen, Ph.D. thesis, Florida State University, 1995.

[11] H. Baer, C-H. Chen, F. Paige, and X. Tata, Phys. Rev. D **52**, 2746 (1995).

[12] While these studies all assume that R parity is conserved, it seems unlikely that there will be no observable signal (especially at linear colliders, but probably even at the LHC [13]) even if this is not the case.

[13] P. Binetrvy and J. Gunion, in *Heavy Flavors and High-Energy Collisions in the 1–100 TeV Range*, Proceedings of the 6th Eloisatron Workshop, Erice, Italy, 1988, edited by A. Ali and L. C. Farelli, Ettore Majorana International Science Series: Physical Sciences Vol. 44 (Plenum, New York, 1989); H. Dreiner, M. Guchait, and D. P. Roy, Phys. Rev. D **49**, 3270 (1994).

[14] M. Chen, C. Dionisi, M. Martinez, and X. Tata, Phys. Rep. **159**, 201 (1988).

[15] J. Feng and D. Finnel, Phys. Rev. D **49**, 2369 (1994).

[16] H. Baer, C-H. Chen, F. Paige, and X. Tata, Phys. Rev. D **50**, 4508 (1994).

[17] H. Baer, M. Drees, C. Kao, M. Nojiri, and X. Tata, Phys. Rev. D **50**, 2148 (1994).

[18] J. Lopez, D. Nanopoulos, G. Park, X. Wang, and A. Zichichi, Phys. Rev. D **50**, 2164 (1994).

[19] T. Kamon, J. Lopez, P. McIntyre, and J. T. White, Phys. Rev. D **50**, 5676 (1994).

[20] H. Baer, C-H. Chen, R. Munroe, F. Paige, and X. Tata, Phys. Rev. D **51**, 1046 (1995).
[21] H. Baer, C-H. Chen, C. Kao, and X. Tata, Phys. Rev. D **52**, 1565 (1995).
[22] S. Mrenna, G. Kane, G. D. Kribbs, and J. D. Wells, Phys. Rev. D **53**, 1168 (1996).
[23] H. Baer, M. Brhlik, R. Munroe, and X. Tata, Phys. Rev. D **52**, 5031 (1995).
[24] F. del Aguila and Ll. Ametller, Phys. Lett. B **261**, 326 (1991).
[25] H. Baer, C-H. Chen, F. Paige, and X. Tata, Phys. Rev. D **49**, 3283 (1994).
[26] R. Barbieri, F. Caravaglios, M. Frigeni, and M. Mangano, Nucl. Phys. **B367**, 28 (1993).
[27] H. Baer, M. Bisset, C. Kao, and X. Tata, Phys. Rev. D **50**, 316 (1994).
[28] F. Paige and S. Protopopescu, in *Supercollider Physics*, edited by D. Soper (World Scientific, Singapore, 1986), p. 41; H. Baer, F. Paige, S. Protopopescu, and X. Tata, in *Proceedings of the Workshop on Physics at Current Accelerators and Supercolliders*, edited by J. Hewett, A. White, and D. Zeppenfeld (Argonne National Laboratory, Agonne, 1993).
[29] While several of these signals have been computed before, we are not aware of a computation of *all* the signals within the SUGRA framework. Such a computation is necessary before we can begin systematic tests of the model.
[30] S. Martin and M. Vaughn, Phys. Lett. B **318**, 331 (1993).
[31] In a previous study [16] of the trilepton signal at the LHC, we had already shown that, with suitable cuts, the contamination from squark and gluino events is small; generating *all* SUSY processes thus greatly reduces the efficiency for these signals, making it essentially impractical to perform even moderately complete scans of the parameter space of the model.
[32] CMS Collaboration, Technical Proposal, No. CERN/LHCC 94-38, 1994 (unpublished).
[33] J. Botts *et al.*, Phys. Lett. B **304**, 159 (1993).
[34] The cross section falls rapidly with the hard scattering p_T, so that if the p_T range is not broken up into smaller intervals, the higher values of $p_T^{\rm HS}$ will not be sufficiently sampled. Since E_T^c is typically 200 GeV, events with relatively small values of $p_T^{\rm HS}$ will not pass the cuts making the computation very inefficient. Breaking up the $p_T^{\rm HS}$ interval into bins will obviously improve the efficacy of the calculation.
[35] W. Beenakker, R. Hopker, M. Spira, and P. Zerwas, Phys. Rev. Lett. **74**, 2905 (1995); Z. Phys. C **69**, 163 (1995).
[36] H. Baer and X. Tata, Phys. Rev. D **47**, 2739 (1993).
[37] V. Barger, Y. Keung, and R. J. N. Phillips, Phys. Rev. Lett. **55**, 166 (1985).
[38] R. M. Barnett, J. Gunion, and H. Haber, Phys. Lett. B **315**, 349 (1993).
[39] H. Dreiner, M. Guchait, and D. P. Roy, Ref. [13]; M. Guchait and D. P. Roy, Phys. Rev. D **52**, 133 (1995).
[40] H. Baer, X. Tata, and J. Woodside, Phys. Rev. D **42**, 1568 (1990).
[41] A. Bartl, W. Majerotto, B. Mösslacher, N. Oshimo, and S. Stippel, Phys. Rev. D **43**, 2214 (1991); A. Bartl, W. Majerotto, B. Mösslacher, and N. Oshimo, Z. Phys. C **52**, 477 (1991); A. Bartl, W. Majerotto, and W. Porod, *ibid.* **64**, 499 (1994).
[42] R. Barbieri and G. Giudice, Nucl. Phys. **B306**, 63 (1988), argue that if SUSY is to ameliorate the fine-tuning problem of the SM, squarks and gluinos should be lighter than $\sim$800 GeV. See G. Anderson and D. Castaño, Phys. Rev. D **52**, 1693 (1995) for an updated measure of fine tuning, and associated limits on sparticle masses.
[43] H. Baer and M. Brhlik, Phys. Rev. D **53**, 597 (1996); see M. Drees and M. Nojiri, *ibid.* **D47**, 376 (1993); G. Kane, C. Kolda, L. Roszkowski, and J. Wells, *ibid.* **49**, 6173 (1994) for related work.
[44] Since our computation of the signals and, especially, backgrounds (which require tails of distributions to be reliably simulated) are uncertain by a factor $\sim$2–3 because of inherent uncertainties associated with our calculation, it could be argued that the reach might be somewhat smaller than that shown in Fig. 18. However, the reader can then make a personal assessment of the reach from the signal cross section contours in Sec. III.
[45] This could, for example, be because unification of scalar (in particular, Higgs boson) masses occurs at a scale slightly different from $M_{\rm GUT}$ as we have assumed. The resulting shift in sfermion masses would not qualitatively change our analysis, but the electroweak symmetry-breaking condition could be significantly modified. For a discussion of this, see M. Olechowski and S. Pokorski, Phys. Lett. B **344**, 201 (1995); N. Polonsky and A. Pomarol, Phys. Rev. D **51**, 6532 (1995).